

Vigo, 5 December 2020

Dear Editor,

We are enclosing the revised version of our manuscript 'Deep maxima of phytoplankton biomass, primary production and bacterial production in the Mediterranean Sea'. The main changes introduced can be summarised as follows:

- *Prochlorococcus* biomass is now included in the calculation of total phytoplankton biomass (Anja Engel and Birthe Zäncker are added as co-authors).
- We have calculated the fucoxanthin:(19'hex-fuco+19'but-fuco) pigment ratio (Fig. S4), which shows that the increase in fucoxanthin at the DCM can be attributed to increased diatom contribution.
- Images from IFCB are included (Fig. S5) to illustrate the distinct composition of phytoplankton in surface and DCM waters and in particular the enhanced presence of diatoms in deep samples.
- Additional information on phytoplankton size structure and water column stability has been added to Table 1.
- The title has been shortened by omitting 'in late spring'. The DCM being persistent throughout the stratification season in the Mediterranean, a reference to sampling time in the title is not required.

Our point-by-point response to the reviewers, including where appropriate an explanation of the changes introduced to the manuscript, is included below.

We will be grateful if our revised manuscript is considered for publication in Biogeosciences.

Sincerely,

Emilio Marañón (on behalf of all coauthors)

Comments by Anonymous Referee #1 and our responses

This is an interesting paper in which the authors discuss the role of photoacclimation and enhanced growth as the underlying mechanism of the DCM in the Mediterranean Sea during the late spring. The study was carried out from 10 May to 11 June during the PEACETIME cruise. The study is exciting; however, I have the following comments/suggestions which will make this manuscript publishable after authors incorporate and modify the paper.

We are grateful to the reviewer for their time and helpful comments.

How can you be sure that the dominance of diatoms at the DCM was resulted from cell sinking from the upper layers due to photoacclimation rather than the new production? I suggest the authors to check any physical mechanism like the role of Rossby wave etc. Analysis of the physical processes in the region is compulsory when you discuss the DCM properties and the underlying mechanism.

We have estimated the diffusive nutrient flux from below the DCM and found that it contributed a small fraction of the nutrient supply required to sustain the deep phytoplankton biomass maximum (see Table 2). In addition, we found no evidence of enhanced phytoplankton growth at the DCM. Hence our conclusion that the DCM was likely to result mainly from cell sinking from above. The role of photoacclimation is supported not only by the strong decrease in C:Chl_a ratios at the DCM but also by the fact that our measurements of PP at the DCM imply higher photosynthetic efficiencies than commonly measured at the DCM in oligotrophic regions where small cells dominate (Uitz et al. 2008).

Planetary Rossby waves have been shown to uplift the DCM (Kawamiya and Oschlies 2001) and cause enhanced surface chlorophyll *a* values (Cippollini et al. 2001) but they are large-scale features that propagate westward over entire ocean basins. Topographic Rossby waves have been observed in the Mediterranean Sea although they are bottom-intensified fluctuations, and therefore not good candidates to explain the occurrence of the DCM. Following the reviewer's advice (see also comment below), we have explored the potential role of other physical mechanisms in originating the DCM. For instance, cells may accumulate in the vertical region of enhanced stability associated with the pycnocline. To explore this possibility, we calculated the depth of maximum Brunt-Väisälä frequency at each long station. We found that the layer of maximum stability lies at a depth of 15-25 m, well above the DCM, which does not support a role for this mechanism during the Peacetime cruise. In the revised version of the manuscript, we have added these data to Table 1, which are referred to in section 3.1 (lines 228-229).

At stations TYRR and FAST, DCM was deeper than nitracline depth. However, DCM was located above the nitracline depth at ION. From this, I understand that the physical processes operating at ION may be different from the other two stations. Hence, insisting to look into the water column stability in all the three stations during the measurement period.

Throughout the cruise, the depth of the DCM and the depth of the nitracline covaried. For the long stations, these two depths differed, on average, by less than 10 m. Indeed the nitracline was deeper than the DCM (on average, by 9 m) at ION whereas the opposite was true in the other long stations, but the actual difference was subtle and it is not clear that it means a different mechanism for DCM formation, particularly in view of the fact that we do not have information on the seasonal dynamics but rely on snapshot observations conducted during a 1-month cruise. Key properties such as the magnitude of the DCM, and the C:Chl_a ratio, phytoplankton growth rate and mean PAR at the DCM were the same at all three stations (see Table 1). As mentioned above, we have also looked into the depth of the maximum Brunt-Väisälä frequency, which was the same at ION and FAST (23 m). The fact that the nitracline was deeper than the DCM at ION probably reflects longitudinal differences in the way the DCM and the mixed layer depth are coupled in the Mediterranean Sea, as discussed by Barbieux et al. (2019). These

authors concluded, from the analysis of seasonal variability in the DCM using Biogeochemical Argo floats data, that in the Ionian and Levantine basins the deepest winter mixed layer rarely reaches the top of the nutricline and the DCM is persistently well above the nutricline during the stratified season. In the revised version of the manuscript, we now refer to this feature in the Discussion (section 4.1, lines 321-325).

In all the three stations, DCM was just below the 1% PAR depth and below the nitracline depth except the station ION; where nitracline depth was deeper than DCM. Have you noticed any difference in phytoplankton characteristics in the DCM at ION compared to the other two? I feel you can make out the difference from the size of the phytoplankton cell. Please check it and confirm that your hypothesis is true in all the three stations. It is also not clear how the individual role of photoacclimation and biomass contribution was explored? Please mention the way to quantify it?

We have calculated, for the three long stations, the mean values of different variables that help to characterize phytoplankton size structure at the DCM: mean cell biovolume (from the imaging flow cytobot), % contribution of cells $> 5 \mu\text{m}$ to total phytoplankton C, and % contribution of cells $> 2 \mu\text{m}$ to total primary production (from size-fractionated PP experiments). This information has been added to Table 1 in the revised manuscript. For all variables, we found no differences between stations, which suggests that, in terms of size structure, the DCM phytoplankton community was comparable among sites. The HPLC pigment data also indicated that in all three stations the contribution of diatoms at the DCM increased markedly in comparison with surface waters, as reflected in the fucoxanthin to total chlorophyll a ratio as well as the fucoxanthin to 19'hex-fuco+19'but-fuco ratio. These data are now shown in the revised version of the manuscript as a new figure in the supplementary information (Fig. S4). The HPLC pigment data did suggest some differences among stations in the upper layers. For instance, within the upper mixed layer of ION and TYRR the phytoplankton assemblage was dominated by prymnesiophytes, followed by cyanobacteria, whereas the opposite was the case at FAST.

To estimate the contribution of photoacclimation (increased Chl per unit C biomass) and increased biomass to explain the DCM, we calculated the DCM to surface ratios for chlorophyll a and phytoplankton C concentration, as explained in section 3.2 of the manuscript. For instance, at station TYRR the deep to surface chl a concentration ratio was 8.14 (0.57/0.07), while the deep to surface ratio in phytoplankton C was 2.17. This means that 26% (2.17/8.14) of the increased chl a at the DCM resulted from enhanced biomass, while the rest of the increased chl a (74%) resulted from photoacclimation. Repeating the same calculations for the other two stations indicates that, overall, photoacclimation accounted for 66-78% of the increase in chl a concentration from the surface to the DCM.

References (not cited in the ms)

- Cippollini et al. (2001) Rossby waves detected in global ocean colour data. *Geophys Res Lett* 28:323-326
- Kawamiya and Oschlies (2001) Formation of a basin-scale surface chlorophyll pattern by Rossby waves *Geophys Res Lett* 28:4139-4142

Comments by Anonymous Referee #2 and our responses

This work reports that the deep chlorophyll maximum (DCM) is a maximum of biomass and primary production in the oligotrophic Mediterranean Sea during late spring. These deep maxima are accompanied by a sub-maximum of bacterial production. The ms is relevant, it reveals that primary production is very significant at the DCM, a component of production undetectable by remote sensing techniques. It is worth mentioning that the biomass data presented are quite new, since the biomass of picoplankton and especially of nanoplankton, the latter seldom directly quantified, were analyzed with specific and appropriate techniques. The ms is well organized and well written and is very easy to read. The figures and tables are clear and explanatory.

We are grateful to this reviewer for their time and helpful comments.

The results may represent a challenge for some current paradigms of phytoplankton ecophysiology. The main factors that regulate phytoplankton growth rates are light, nutrients and temperature. The study concludes that growth rates remain more or less constant along the water column. Between the surface layers and the DCM, irradiance decreases from saturating to limiting conditions and temperature decreased about 5 C in this study. These two factors alone should have significantly decreased phytoplankton growth rates at the DCM, which could have been compensated somehow by an increase of diffusive nutrient supply to the DCM from the nutricline. However, the measured nutrient supply was low. The authors explain their findings by the presence of a diatom community in the DCM layer that was very efficient at low irradiances (I would add temperature). The implications would be important since these results show that composition conditions the phytoplankton response, which should question general ecophysiological assumptions that are often extrapolated to natural conditions by some models. The following are some issues that I suggest be examined further to reinforce the important findings of the study (sentences copied from the ms are signaled between quotation marks)

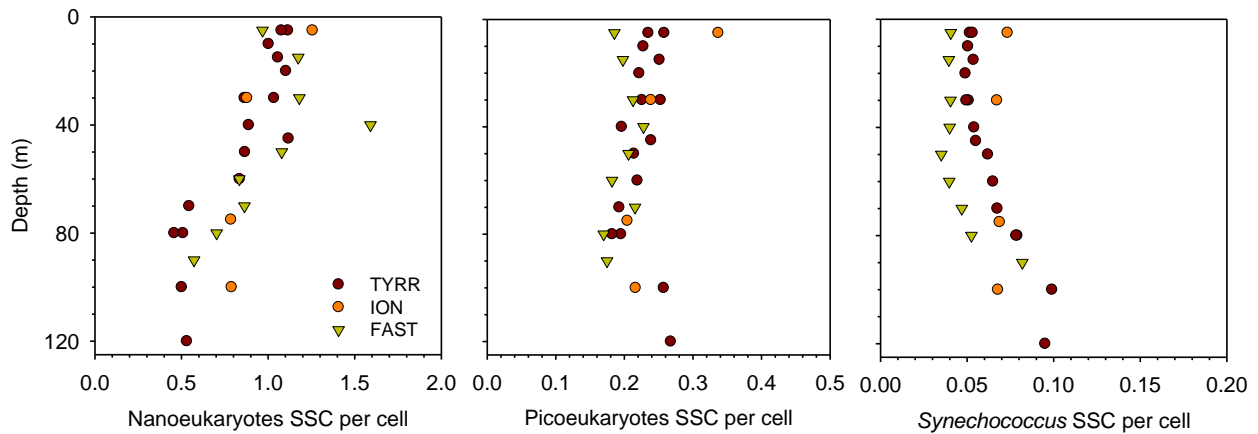
The observation that phytoplankton growth rates were rather invariant across the euphotic layer does seem counterintuitive in the face of strong gradients in irradiance and temperature. However, the same pattern (i.e. similar growth rates in the surface layer and near the base of the euphotic layer) has often been reported by other studies, such as (cited in the ms) Pérez et al. (2006) and Berthelot et al. (2019) and also (not cited in the ms) Cáceres et al. (2013), Landry et al. (2004) and Armengol et al. (2019). Specifically, Cáceres et al. (2013) found virtually the same growth rate throughout the euphotic layer in a station located in the eastern subtropical North Atlantic (their Fig. 7, bottom panels). Landry et al. (2004) measured the same growth rate at the surface and at 60 m in an offshore oligotrophic station off Southern California (their Fig. 2, Cruise P0605 Cycle 5). Armengol et al. (2019) reported (their Table 2, stations 1-7) a mean growth rate of $0.28 \pm 0.18 \text{ d}^{-1}$ at the surface compared with $0.21 \pm 0.07 \text{ d}^{-1}$ at the DCM in the central tropical Atlantic. In the revised version of the manuscript, we have added a reference to these additional studies in the Discussion (section 4.3) (line 445).

The paradox of relatively constant phytoplankton growth throughout the euphotic layer in oligotrophic settings can perhaps be explained by considering that the physiological effect of a given environmental factor tends to decrease when another factor is limiting. Most laboratory experiments are designed to determine the effect of a single environmental driver while keeping other variables under optimal levels. For instance, under nutrient-sufficient conditions the effect of irradiance on growth is strong, and under optimal nutrient and irradiance conditions the effect of temperature is also strong. However, the temperature dependence of phytoplankton growth is greatly reduced under conditions of light (Edwards et al. 2016) or nutrient (Marañón et al. 2018) limitation. Conversely, the effect of increasing nutrient supply on growth is modest when temperatures are strongly limiting (see review by Cross et al. 2015). Thus the lack of irradiance effects on the growth rate of acclimated phytoplankton assemblages may result from the

fact that nutrient limitation prevails throughout the water column. We have added this suggestion to section 4.3 in the revised version of the manuscript (lines 448-453).

Carbon estimates Estimates of C biomass are paramount in this work. More accurate biovolume estimates can be obtained using the scattering properties (forward or side scattering) of single cells than by assuming mean volumes for picoplankton and nanoplankton. In addition, this procedure would take into account the important changes of cell size with depth, often ignored (Binder et al. 1996. Dynamics of picophytoplankton, ultraphytoplankton and bacteria in the central equatorial Pacific. Deep. Res. II 43: 907-931, Mena et al 2019, cited by the authors).

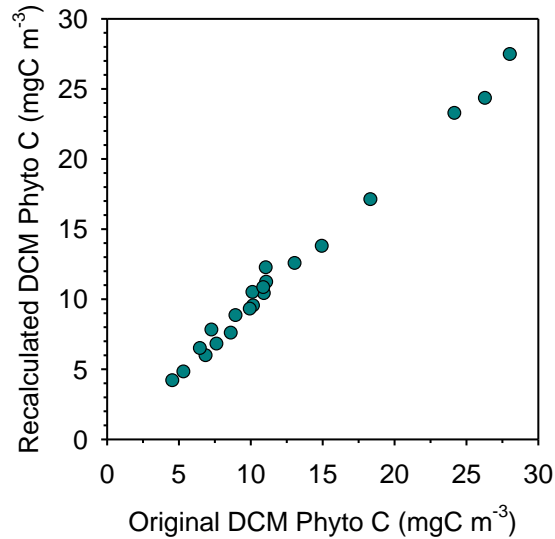
Although estimates of cell biovolume based on the side scattering (SSC) signal were not routinely available for the cruise, we have examined a few profiles of SSC per cell at the long stations to assess depth-related changes in cell biovolume of *Synechococcus*, picoeukaryotes and nanoeukaryotes. As shown in the plots and table below, we found that cell biovolume of nano- and pico-eukaryotes decreased with depth whereas the opposite was true for *Synechococcus*.



Mean (and standard deviation) of the side-scattering signal per cell of different groups in the surface layer (0-40 m) and at the DCM (including also the sample obtained immediately above the DCM) in the three long stations (data from all stations were pooled together).

	SSC per cell		
	Nanoeukaryotes	Picoeukaryotes	<i>Synechococcus</i>
Surface (n = 13)	1.06 (0.11)	0.24 (0.04)	0.052 (0.010)
DCM (n = 11)	0.64 (0.15)	0.21 (0.03)	0.074 (0.017)

We have recalculated the total biomass of phytoplankton at the DCM taking into account these depth-related changes in cell volume of pico and small nanophytoplankton. Specifically, the value of C biomass per cell used in the original calculations was multiplied by the observed DCM to surface SSC ratio for each group, which was 0.61 for nanoeukaryotes, 0.87 for picoeukaryotes and 1.42 for *Synechococcus*. The figure below shows that taking into account these changes in cell volume with depth has negligible effects on the estimated total phytoplankton biomass at the DCM:



Please, specify the volume analyzed for detecting a significant number of cells from the small nanophytoplankton fraction, it is an interesting information that can help other researches and future studies.

Samples were run at a flow rate of $145 \mu\text{L min}^{-1}$ for 5 min so that analysed volume for each sample was $725 \mu\text{L}$. This information is now included in section 2.3 of the revised manuscript (lines 137-138).

L. 138. "Thus the increase, from the surface to the base of the euphotic layer, in phytoplankton biomass was ca. 2-fold, compared with ca. 8-fold for TChl a." Please, consider recalculating the biomass taking into account changes of biovolume with depth.

As shown in the response above, when phytoplankton biomass at the DCM is recalculated taking into account depth-related changes in SSC the new biomass data are virtually identical to the original ones. This results from several factors: i) the vertical changes in cell volume of picoeukaryotes were minor, ii) the change of *Synechococcus* and that of nanoeukaryotes were substantial but showed opposite trends, thus counterbalancing each other, and iii) the biomass of all groups measured with flow cytometry represent, on average, $\leq 40\%$ of total phytoplankton biomass at the DCM.

Diatoms at the DCM L. 264. "The fucoxanthin to total chlorophyll a ratio (Fuco: TChl a) consistently increased below the upper 40-50 m in all long stations." From the changes in this ratio it is deduced that diatom contribution increases with depth. Fucoxanthin is also present in haptophytes and pelagophytes, two main components of phytoplankton with 19'hex-fuco and 19'but-fuco as their main diagnostic pigments, respectively. To make sure the increase in fucoxanthin is due to diatoms I would recommend calculating the vertical distribution of fucoxanthin: (19'hex-fuco + 19'but-fuco). The increase of this ratio with depth would be a more convincing evidence of a differential increase in diatoms. The images obtained with the Imaging Flow CytoBot should help to confirm that diatoms dominated or were very abundant in the DCM layer.

Following the reviewer's advice, we have calculated the fucoxanthin:(19'hex-fuco+19'but-fuco) ratio and verified that it increases consistently with depth. In fact, the vertical distribution of the fucoxanthin:(19'hex-fuco+19'but-fuco) ratio is nearly identical to that of the fucoxanthin:chlorophyll a ratio, which supports our conclusion of increased diatom contribution at the DCM. The new pigment ratio is now reported in the supplementary information of the revised manuscript (Fig. S4). We have also included mosaics of all cells imaged by the IFCB in surface and DCM samples from the three long

stations. These mosaics show that diatoms were abundant at the DCM of all three stations and virtually absent in surface samples (new Fig S5). The new pigment profiles and the IFCB images are described in the Results section of the revised manuscript (lines 284-288).

L. 375. ": :this trend was associated with a significant increase in the contribution of diatoms to total phytoplankton biomass, which reached at least 30 % in the DCM of all stations, and was particularly high (nearly 50 %) in the most stratified station, located in the Ionian Sea." Please, re-check your estimates of diatom contribution at the DCM. Although I agree that diatoms can increase at the DCM, these values appear very high. In addition, the data of Crombet et al 2011 (cited in ms) show a patchy distribution of the Deep Silica Maximum and diatoms in the DCM of the Mediterranean.

It has to be noted that our cruise took place during late spring whereas the survey reported by Crombet et al. (2011) was conducted in summer, more than 1.5 months later in the year. We estimated the diatom contribution to total chl a by using three different pigment coefficients. The lowest pigment coefficient used (1.41, taken from Uitz et al. 2006), which gives a lower-bound estimate of diatom contribution, is derived from a large database covering a broad range of trophic situations and including the entire water column, not just the surface layer as is typically the case. We therefore consider that the resulting estimate of diatom contribution is robust. Note that station ION, which has the highest estimated contribution of diatoms in the DCM, is also the one that shows the highest abundance of diatoms in the IFCB images (new Fig. S5).

Primary production (PP) at the DCM L. 309. "In contrast, during PEACETIME the mean depths of the primary production maximum and the DCM coincided and only on 3 profiles was the primary production peak located above the DCM." The subsequent discussion does not present potential mechanisms to explain the discrepancy in PP estimates at the DCM between this and previous studies cited in the ms, which show a PP maximum above the DCM most of the time. It does argue that the high primary production at the DCM during PEACETIME was due not only to enhanced levels of phytoplankton biomass but also to the presence of a diatom-rich community characterized by high photosynthetic efficiency. It is a bit surprising that the same response has not been found in previous studies in the area. Could it be possible that the presence of diatoms with high photosynthetic efficiency at the DCM discussed by the authors is a consequence of the previous spring bloom at the surface and not a regular feature of the DCM in the Mediterranean? Estrada et al (1993. Variability of deep chlorophyll maximum characteristics in the Northwestern Mediterranean. Mar. Ecol. Prog. Ser. 92: 289–300) reported the occasional presence of diatoms from a decaying bloom that contributed significantly to the DCM biomass but with a very low photosynthetic efficiency, which seems typical of sinking cells. It seems that a large contribution of diatoms in the DCM layer is not a general feature of the Mediterranean Sea, and perhaps could explain the discrepancies in PP estimates at this depth with other studies.

We agree with the reviewer that the high diatom abundance and productivity observed during our cruise are not necessarily persistent features of the DCM in the Mediterranean sea. In fact, we end the Conclusions section by pointing out that future, high-resolution studies are needed to ascertain if the observed peak in productivity is a persistent feature of the DCM in the Mediterranean Sea. It may well be the case that, as indicated by the reviewer, the significant biomass contribution of diatoms observed at the DCM results from the sedimentation of the earlier spring bloom. In the revised version of the manuscript, we acknowledge that 1) our results have a limited temporal coverage and therefore cannot be used to ascertain if the deep productivity maxima are persistent during the stratification season and 2) it is possible that the enhanced biomass contribution of diatoms at the DCM results in part from the sedimentation of the spring bloom prior to the cruise (lines 408-411).

L. 340. "In contrast, during our survey the contribution of increased phytoplankton biomass was similar in all stations, including the one located in the Ionian Sea." An important conclusion is that DCM is a maximum of biomass and production in the Mediterranean, at least during the period of the study. However, in 3 of the 4 profiles obtained in the Tyrrhenian Sea the biomass maximum is well above the DCM. This result is mentioned (line 235) but ignored throughout the ms. Moreover, it is difficult to explain how the PP maximum can be found at 70-80m, at the DCM and below the biomass maxima in these stations without a significant increase of nutrient supply. The correction that has been applied to short-term temperature variations to estimate PP at in-situ temperature from incubations at higher temperatures (about 5 C) could be discussed further to see if they may have distorted the results of the deep layers.

The biomass profiles have been modified in the revised manuscript as a result of the inclusion of *Prochlorococcus*, which was abundant in the DCM. The TYRR profile obtained on 18 May shows an increased biomass at both 45 m and 80 m, whereas the profile on 19 May shows increased biomass only at 50 m. It has to be noted that the magnitude of the deep PP peaks is minor in both these profiles. The rates of primary production measured at the DCM are only slightly higher than those measured at the surface (2 vs 1.7 and 3 vs 2.3 mgC m⁻³ d⁻¹, respectively). On 17 May, PP at the DCM was twice as large as that at the surface, but biomass was also higher by a factor of 3. Large discrepancies between biomass and primary production would have resulted in anomalous values of biomass turnover rates, which were not found. The temperature correction used assumes a strong sensitivity of photosynthesis to temperature ($E_a = 0.61$ eV, approximately equivalent to $Q_{10} = 2.3$), which only moderates the magnitude of the deep PP peaks. This was already explained in the first version of the manuscript (section 4.1).

L. 444. "Thus the surface BP (bacterial production) peak observed under in situ conditions was not due to dependence of organic carbon substrates but may have resulted in part from new N and P availability through dry atmospheric deposition." This explanation can be applied to phytoplankton as well. If atmospheric input of inorganic nutrients and recycling are the main reasons for vertical patterns of bacterial production, the same pattern should have been found for primary production (which is the pattern usually found by other studies in the Mediterranean cited in the ms).

The response to atmospheric deposition may not be necessarily symmetrical between phytoplankton and heterotrophic bacteria, as the latter tend to respond faster and more intensely to the nutrients injected from the atmosphere (see review of dust addition bioassays in Guieu et al. 2014). In fact, the superior ability of heterotrophic bacteria to compete for inorganic nutrients has been shown by the budget analysis and experimental observations of Van Wambeke et al. (2020), who concluded that dry atmospheric deposition could supply nearly 40% of the heterotrophic bacteria N demand in the upper mixed layer. A reference to this result has been added to the Discussion (section 4.4, lines 477-481)

L. 335. "Therefore low nutrient availability, which is widespread in the global ocean (Moore et al., 2013), results not only in low phytoplankton biomass but also in slow growth rates." This conclusion is controversial in the scientific community. Another line of research with direct estimates of growth rates using mainly dilution experiments argue that, even with low nutrient concentrations, fast supply of nutrients from recycling results in the predominance of phytoplankton, usually of small size, with relatively high growth rates (Laws, E. A., 2013. Evaluation of in situ phytoplankton growth rates: A synthesis of data from varied approaches. *Ann. Rev. Mar. Sci.* 5: 247–268, and ref therein), although lower than those of taxa typical for bloom situations. Different optimal growth rates can be a function of taxonomical affiliation or size, among other reasons.

Other results from dilution experiments, not cited by Laws (2013), show that slow growth rates prevail in low-productivity waters. For instance, Landry et al. (2008) measured rates around 0.3 d⁻¹ in oligotrophic waters off Hawaii not affected by a cyclonic eddy, while finding rates as high as 0.6 d⁻¹ in stations inside

the eddy. In another study, Landry et al. (2009) found euphotic layer-integrated phytoplankton growth rates of 0.1-0.2 d⁻¹ in oceanic, well-stratified stations off southern California, compared with rates of 0.2-0.5 d⁻¹ in stations within the coastal upwelling region (their Fig. 3). More recently, Armengol et al. (2019) obtained (also with the dilution method) mean growth rates around 0.3 d⁻¹ across the oligotrophic tropical Atlantic (10°N-0°S). These additional references are now cited in the Discussion of the revised manuscript (section 4.1, lines 352-353)

We agree with the reviewer that different taxa have different maximum growth rates. However, even though some strains of *Prochlorococcus* and *Synechococcus* may have relatively low maximum growth rates (<0.5 d⁻¹), picoeukaryotes of wide distribution such as *Ostreococcus* sp. and *Micromonas* sp. can indeed grow at rates ≥ 0.5 d⁻¹ (Six et al. 2008, Demory et al. 2019). The results of Berthelot et al. (2018) that we cite are especially relevant because they were based on measurements of isotope uptake by intact, single cells, thus avoiding some of the uncertainties involved in bulk methods. They found that growth rates of picoeukaryotes were 0.15-0.26 d⁻¹ in the North Pacific subtropical gyre compared with 0.42-0.50 d⁻¹ in stations within the California coastal current. Also, in situ experiments in HNLC waters have shown unequivocal increases in growth rates once Fe limitation was removed (Boyd et al. 2008). Finally, flow cytometry measurements of single-cell fluorescence (a proxy for abundance of photosynthetic units) in subtropical gyres (Davey et al. 2008, Browning et al. 2017) show that investment in photosynthetic machinery increases markedly after nutrient addition, again supporting the view that nutrient limitation in oligotrophic regions causes physiological impairment and thus reduced growth rate.

Keep the same y-scale for fig 3g, h and i.

The scale in Fig 3i has been changed accordingly.

References (not cited in the ms)

Armengol et al. (2019) Planktonic food web structure and trophic transfer efficiency along a productivity gradient in the tropical and subtropical Atlantic Ocean. *Sci Rep* 9, Article No 2044

Boyd et al. (2008) Mesoscale Iron Enrichment Experiments 1993-2005: Synthesis and Future Directions *Science* 315 :612-617

Browning et al. (2017) Nutrient co-limitation at the boundary of an oceanic gyre. *Nature*, doi:10.1038/nature24063.

Cáceres et al. (2013) Phytoplankton Growth and Microzooplankton Grazing in the Subtropical Northeast Atlantic. *PlosOne* 8(7) e69159.

Davey et al. (2008) Nutrient limitation of picophytoplankton photosynthesis and growth in the tropical North Atlantic. *Limnol Oceanogr* 53:1722-1733.

Demory et al. (2019) Picoeukaryotes of the *Micromonas* genus: sentinels of a warming ocean. *The ISME Journal*, 13:132-146

Edwards et al. (2016) Phytoplankton growth and the interaction of light and temperature: A synthesis at the species and community level. *Limnol Oceanogr*, doi: 10.1002/lno.10282

Landry et al. (2008) Depth-stratified phytoplankton dynamics in Cyclone Opal, a subtropical mesoscale eddy. *Deep Sea Res* 55:1348-1359

Landry et al. (2009) Lagrangian studies of phytoplankton growth and grazing relationships in a coastal upwelling ecosystem off Southern California. *Prog Oceanogr* 83:208-216

Six et al. (2008) Contrasting photoacclimation costs in ecotypes of the marine eukaryotic picoplankter *Ostreococcus*. *Limnol Oceanogr* 53:255

Van Wambeke et al. (2020) Influence of atmospheric deposition on biogeochemical cycles in an oligotrophic ocean system. *Biogeosciences*, under revision.

Comments by Anonymous Referee #3 and our responses

This MS addresses the ubiquitous subsurface feature, the deep chlorophyll maximum, phytoplankton biomass and production, and heterotrophic prokaryotic production in the Mediterranean sea's stratified water column during the later spring season (May 10, 2017- June 11, 2017). This subsurface feature in the world ocean is known for long, more prominent in waters of lower latitude, are often found at nutricline depth well below the remote sensing reach, thus supports the importance of seaboard measurements to capture this feature. Chlorophyll a, an indicator of the phytoplankton biomass, is regulated by light, nutrient, etc. Here, the authors mainly aim to quantify photoacclimation's relative role and enhanced growth as an essential DCM mechanism. Secondly, the trophic coupling between phytoplankton and heterotrophic prokaryotic production is also addressed. Based on shipboard measurements in the Mediterranean sea, authors conclude that the DCM located at subsurface depth coincides with both biomass and primary production but not in growth rate and explains that the photoacclimation process leads to the increased chlorophyll a at the DCM. This study contributes vital insight into likely future ocean changes under the ocean warming scenario, thus merits publication of this work. However, I do not recommend a journal publishing this work in the present form. A few concerns about the methodology and the data interpretation need to be taken care of before considering this work for publication (see below).

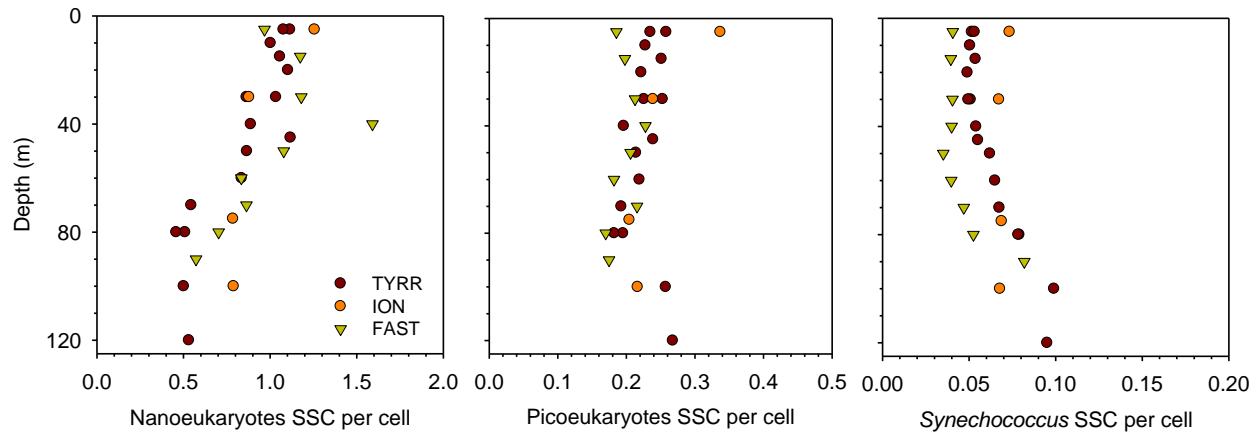
We are grateful to this reviewer for their time and helpful comments.

Flow cytometry tool followed to obtain estimates of the carbon biomass in different size categories does not seem to have taken account of the autotrophic cells >150 microns in size neither their contribution is quantified, if minimal. The authors could have easily viewed these samples (>150micron) under the microscope to support the finding. If this were a significant observed, increased carbon biomass from the surface to the euphotic layer base would have been different and could lead to a different conclusion. The authors need to take care of this part in the section result and subsequently draw a conclusion at the end of the discussion section.

Although a 150- μm mesh is used to pre-filter the samples, particles with a length >150 μm can still be imaged by the IFCB. These include elongated, single cells (such as *Rhizosolenia* sp.) and diatom chains, both of which can be seen in the mosaics that are now shown in the revised manuscript (Fig. S5). Size-abundance spectra obtained with microscopy image analysis in oligotrophic waters indicate that cells with a volume of $\geq 10,000 \mu\text{m}^3$ (assuming a cylindrical, elongated shape such as that of *Rhizosolenia*, this volume corresponds roughly to cells with a length of 150 μm and a diameter of 10 μm) contribute on average approximately 1% of total biovolume (Huete-Ortega et al. 2011, Marañón 2015). It is thus unlikely that the IFCB has significantly underestimated the total community biovolume. Being a methodological issue, this point is clarified in the Methods of the revised manuscript (section 2.3, lines 154-158).

Also, it is unclear whether definite size beads were run on flow cytometry to conclude the mean cell diameter used for carbon calculation. It is essential to show the reader the error introduced by assuming the mean cell diameter (2 μm or 4 μm or 6 μm).

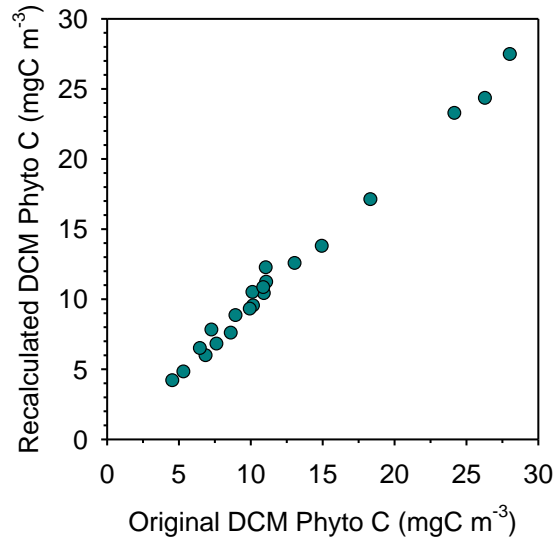
As explained in the Methods section, C biomass estimates for small phytoplankton (measured with flow cytometry) assumed constant C content for each group of cells. Although estimates of cell biovolume based on the side scattering (SSC) signal were not routinely available for the cruise, we have examined a few profiles of SSC per cell at the long stations to assess depth-related changes in cell biovolume of *Synechococcus*, picoeukaryotes and nanoeukaryotes. As shown in the plots and table below, we found that cell biovolume of nano- and pico-eukaryotes decreased with depth whereas the opposite was true for *Synechococcus*.



Mean (and standard deviation) of the side-scattering signal per cell of different groups in the surface layer (0-40 m) and at the DCM (including also the sample obtained immediately above the DCM) in the three long stations (data from all stations were pooled together).

	SSC per cell		
	Nanoeukaryotes	Picoeukaryotes	<i>Synechococcus</i>
Surface (n = 13)	1.06 (0.11)	0.24 (0.04)	0.052 (0.010)
DCM (n = 11)	0.64 (0.15)	0.21 (0.03)	0.074 (0.017)

We have recalculated the total biomass of phytoplankton at the DCM taking into account these depth-related changes in cell volume of pico and small nanophytoplankton. Specifically, the value of C biomass per cell used in the original calculations was multiplied by the observed DCM to surface SSC ratio for each group, which was 0.61 for nanoeukaryotes, 0.87 for picoeukaryotes and 1.42 for *Synechococcus*. The figure below shows that taking into account these changes in cell volume with depth has negligible effects on the estimated total phytoplankton biomass at the DCM:



On the other hand, while calculating Fucoxanthin to total chlorophyll a ratio calculation, I find authors have ignored that besides diatoms, *Phaeocystis* spp. are also potential sources of Fucoxanthin (see Latasa and Bidigare, 1998) instead accounted to diatom community.

To examine the possibility that the increase in fucoxanthin with depth may have reflected an increased abundance in other fucoxanthin-containing groups such as haptophytes and pelagophytes, we have calculated the fucoxanthin:(19'hex-fuco+19'but-fuco) ratio. We found that the vertical distribution of the fucoxanthin:(19'hex-fuco+19'but-fuco) ratio is nearly identical to that of the fucoxanthin:chlorophyll a ratio, which supports our conclusion of increased diatom contribution at the DCM. The new pigment ratio is now shown in the supplementary information of the revised manuscript (Fig. S4). We have also added the mosaics of all cells imaged by the IFCB in surface and DCM samples from the three long stations. These mosaics show that diatoms were abundant at the DCM of all three stations and virtually absent in surface samples (new Fig S5).

Furthermore, the presence of divinyl chl a, a marker for prochlorophyte, seems to have ignored and accounted for diatoms. Suggest authors revisit HPLC based pigment (depth-wise) analyses to rule out Prochlorococcus community is not missed out. In my opinion, low light-adapted Prochlorococcus at the DCM may be sizably contributing to the DCM community.

Following the reviewer's advice, we have assessed the potential contribution of *Prochlorococcus* to total phytoplankton biomass with previously unused data obtained with flow cytometry. Applying a cell C content of 0.06 pgC cell⁻¹ (based on Buitenhuis et al. 2012), the typical *Prochlorococcus* abundances measured at the DCM (ca. 40,000 cell mL⁻¹) represent a C biomass of ca. 2.4 mgC m⁻³. By contrast, *Prochlorococcus* was undetected in the upper layers (0-30 m). In the revised version of the manuscript, total phytoplankton biomass has been recalculated taking into account also the contribution of *Prochlorococcus* (Figs. 3d,e,f and S2b).

References

- Marañón (2015) Cell size as a key determinant of phytoplankton metabolism and community structure. *Annual Review of Marine Science*, 7, 241-264. doi: 10.1146/annurev-marine-010814-015955
- Huete-Ortega et al. (2011) Isometric size-scaling of metabolic rate and the size abundance distribution of phytoplankton. *Proceedings of the Royal Society B*, 279, 1815-1823. doi:10.1098/rspb.2011.2257.

Deep maxima of phytoplankton biomass, primary production and bacterial production in the Mediterranean Sea during late spring

Emilio Marañón¹, France Van Wambeke², Julia Uitz³, Emmanuel S. Boss⁴, Céline Dimier³, Julie Dinasquet⁵, Anja Engel⁶, Nils Haëntjens⁴, María Pérez-Lorenzo¹, Vincent Taillandier³, Birthe Zäncker^{6,7}

¹Department of Ecology and Animal Biology, Universidade de Vigo, 36310 Vigo, Spain

²Aix-Marseille Université, CNRS, Université de Toulon, CNRS, IRD, Mediterranean Institute of Oceanography, MIO UM 110, 13288 Marseille, France

³CNRS and Sorbonne Université, Laboratoire d'Océanographie de Villefranche, 06230 Villefranche-sur-mer, France

⁴School of Marine Sciences, University of Maine, Orono, Maine, USA

⁵Scripps Institution of Oceanography, University of California, San Diego, USA

⁶GEOMAR, Helmholtz Centre for Ocean Research Kiel, 24105 Kiel, Germany

⁷Marine Biological Association of the UK, Plymouth, PL1 2PB, United Kingdom

Correspondence to: E. Marañón (em@uvigo.es)

Abstract

The deep chlorophyll maximum (DCM) is a ubiquitous feature of phytoplankton vertical distribution in stratified waters that is relevant for our understanding of the mechanisms that underpin the variability in photoautotroph ecophysiology across environmental gradients and has implications for remote sensing of aquatic productivity. During the PEACETIME (*Process studies at the air-sea interface after dust deposition in the Mediterranean Sea*) cruise, carried out from 10 May to 11 June 2017, we obtained 23 concurrent vertical profiles of phytoplankton chlorophyll *a*, carbon biomass and primary production, as well as heterotrophic prokaryotic production, in the western and central Mediterranean basins. Our main aims were to quantify the relative role of photoacclimation and enhanced growth as underlying mechanisms of the DCM and to assess the trophic coupling between phytoplankton and heterotrophic prokaryotic production. We found that the DCM coincided with a maximum in both biomass and primary production but not in growth rate of phytoplankton, which averaged 0.3 d⁻¹ and was relatively constant across the euphotic layer. Photoacclimation explained most of the increased chlorophyll *a* at the DCM, as the carbon to chlorophyll *a* ratio (C:Chl *a*) decreased from ca. 90-100 (g:g) at the surface to 20-30 at the base of the euphotic layer, while phytoplankton carbon biomass increased from ca. 6 mgC m⁻³ at the surface to 10-15 mgC m⁻³ at the DCM. As a result of photoacclimation, there was an uncoupling between chlorophyll *a*-specific and carbon-specific productivity across the euphotic layer. The fucoxanthin to total chlorophyll *a* ratio increased markedly with depth, ~~as did the biomass contribution of large cells,~~ suggesting an increased contribution dominance of diatoms at the DCM. The increased biomass and carbon fixation at the base of the euphotic zone was associated with enhanced rates of heterotrophic prokaryotic activity, which also showed a surface peak linked with warmer temperatures. Considering the phytoplankton biomass and turnover rates measured at the DCM, nutrient diffusive fluxes across the nutricline were able to supply only a minor fraction of the photoautotroph nitrogen and phosphorus requirements. Thus the deep maxima in biomass and primary production were not fueled by new nutrients, but likely resulted from cell sinking from the upper layers in combination with the high photosynthetic efficiency of a diatom-rich, low-light acclimated community largely sustained by regenerated nutrients. Further studies with increased temporal and spatial resolution will be required to ascertain if the deep primary production peaks associated with the DCM persist across the western and central Mediterranean Sea throughout the stratification season.

1. Introduction

42 One of the most remarkable features of phytoplankton distribution in lakes and oceans is the presence of a deep
chlorophyll maximum (DCM), typically located at the base of the euphotic layer and coinciding with the top of the
44 nutricline, that occurs in permanently and seasonally stratified water columns (Herbland and Voituriez, 1979; Cullen,
2015). Multiple, non-mutually exclusive mechanisms may contribute to the development of a DCM, including
46 photoacclimation (the increase in cellular chlorophyll content as a response to low light conditions) (Geider, 1987),
enhanced growth conditions at the layer where elevated nutrient diffusion from below coexists with still sufficient
48 irradiance (Beckmann and Hense, 2007), a decrease in sinking rates near the pycnocline (Lande and Wood, 1987), and
changes in buoyancy regulation or swimming behaviour of cells (Durham and Stocker, 2012). Photoacclimation is a
50 rapid process that takes place in a matter of hours (Fisher et al., 1996), and therefore part of the increased chlorophyll
concentration at the DCM is always the result of a decrease in the phytoplankton carbon to chlorophyll *a* ratio (C:Chl
52 *a*), which results mainly from decreased irradiance but is also favoured by enhanced nutrient supply (Geider et al.,
1996). Although the role of photoacclimation, particularly in strongly oligotrophic environments, has long been
54 acknowledged (Steele, 1964), the fact that Chl *a* is used routinely as a surrogate for photoautotrophic biomass has
helped to fuel the assumption, often found in the scientific literature and in textbooks, that the DCM is always a
56 maximum in the biomass and, by extension, the growth rate of phytoplankton. The assessment of total phytoplankton
biomass along vertical gradients has been traditionally hindered by the time-consuming nature of microscopy
58 techniques, but the increasing use of optical properties such as the particulate beam attenuation and backscattering
coefficients to estimate the concentration of suspended particles in the water column (Martinez-Vicente et al., 2013;
60 Behrenfeld et al., 2016) has allowed to characterize biogeographic and seasonal patterns in the vertical variability of
phytoplankton chlorophyll and biomass in stratified environments (Fennel and Boss, 2003; Mignot et al., 2014; Cullen,
62 2015).

It is now established that the nature of DCM changes fundamentally along a gradient of thermal stability and nutrient
64 availability (Cullen, 2015). In the oligotrophic extreme, represented by permanently stratified regions such as the
subtropical gyres, the DCM is mostly a result of photoacclimation and does not constitute a biomass maximum
66 (Marañón et al., 2000; Pérez et al., 2006; Mignot et al., 2014). However, a biomass maximum, located at a shallower
depth than the DCM, can develop in oligotrophic conditions as a result of the interplay between phytoplankton growth,
68 biological losses and sinking (Fennel and Boss, 2003). In mesotrophic regimes, such as seasonally stratified temperate
seas during summer, the DCM is often also a biomass maximum that manifests as a peak in beam attenuation or
70 backscattering (Mignot et al., 2014). Both ends of this trophic gradient can be found in the Mediterranean Sea along its
well-known longitudinal trend in nutrient availability, phytoplankton biomass, and productivity (Antoine et al., 1995;
72 D'Ortenzio and Ribera d'Alcalà, 2009; Lavigne et al., 2015). Using data from biogeochemical Argo (BGC-Argo)
profiling floats deployed throughout the Mediterranean, (Barbieux et al., 2019) established general patterns in the
74 distribution and seasonal dynamics of biomass (estimated from the particulate backscattering coefficient) and
chlorophyll subsurface maxima. They found that in the western Mediterranean Sea, during late spring and summer, a
76 subsurface biomass maximum develops that coincides with a chlorophyll maximum and is located roughly at the same
depth as the nutricline and above the $0.3 \text{ mol quanta m}^{-2} \text{ d}^{-1}$ isolume. In contrast, in the Ionian and Levantine seas the
78 DCM, which has a smaller magnitude, arises solely from photoacclimation and is located well above the nutricline at a
depth that corresponds closely with the $0.3 \text{ mol quanta m}^{-2} \text{ d}^{-1}$ isolume (Barbieux et al., 2019). The presence of a
80 subsurface or deep biomass maximum may suggest that a particularly favourable combination of light and nutrients
occurs at that depth, leading to enhanced phytoplankton growth and new production. It remains unknown, however,

82 whether phytoplankton growth and biomass turnover rates are actually higher at the depth of the biomass maximum. An
83 additional source of uncertainty is that both the particulate attenuation and backscattering coefficients relate not only to
84 phytoplankton abundance but to the entire pool of particles, including non-algal and detrital particles, which are known
85 to contribute significantly to total suspended matter in oligotrophic regions (Claustre et al., 1999). Combining direct and
86 specific measurements of phytoplankton production (with the ^{14}C -uptake technique) and biovolume (with flow
87 cytometry) offers a way to determine photoautotrophic biomass turnover rates (Kirchman, 2002; Marañón et al., 2014)
88 and thus gain further insight into the dynamics and underlying mechanisms of the DCM. By investigating concurrently
89 the vertical variability in heterotrophic prokaryotic production in relation to phytoplankton standing stocks and
90 productivity, it is also possible to ascertain potential implications of the DCM for trophic coupling within the microbial
91 plankton community.

92 The PEACETIME (*Process studies at the air-sea interface after dust deposition in the Mediterranean Sea*) cruise,
93 which investigated atmospheric deposition fluxes and their impact on biogeochemical cycling in the Mediterranean Sea
94 (Guieu et al., 2020), covered the Western, Tyrrhenian and Ionian regions during late spring 2017, when the DCM was
95 already well developed. Here we describe the vertical variability in chlorophyll *a* concentration, phytoplankton biomass
96 and production, and heterotrophic prokaryotic production. Our main goals are: 1) to determine the extent to which
97 photoacclimation, enhanced phytoplankton biomass, and enhanced productivity and growth underlie the DCM; 2) to
98 characterize the vertical variability in C:Chl *a*, and C biomass-specific and Chl *a*-specific production, and 3) to assess
99 the trophic coupling between phytoplankton photosynthetic activity and heterotrophic bacterial production. The results
100 presented provide a context, in terms of the abundance and activity of key microbial plankton groups, to other
101 ecological and biogeochemical investigations carried out during the PEACETIME cruise and included in this special
102 issue.

2. Methods

2.1 Oceanographic cruise

104 A detailed description of the ensemble of atmospheric and oceanographic observations conducted during the
105 PEACETIME process study can be found in Guieu et al. (2020). Here we report measurements conducted during an
106 oceanographic cruise on board the *R/V Pourquoi Pas?*, which took place in the western and central Mediterranean Sea
107 during the period 10 May – 11 June 2017 (Fig. 1). The cruise focused on three long-stay stations, which were occupied
108 during 4-5 days: station TYRR, located in the Tyrrhenian Sea (39° 20.4' N, 12° 35.6' E); station ION, located in the
109 Ionian Sea (35° 29.1' N, 19° 47.8' E); and station FAST, located in the Balearic Sea (37° 56.8' N, 2° 54.6' E). The
110 latter station was occupied as part of a fast-action response to investigate the biogeochemical impacts of an event of
111 atmospheric wet deposition that occurred during the period 3-5 June (Guieu et al., 2020). In addition, 10 short-stay
112 stations were occupied during 8 hours. At all stations, CTD casts were conducted and seawater samples obtained for the
113 measurement of the abundance, biomass and productivity of phytoplankton and bacterioplankton.
114

2.2 Sampling, hydrography and irradiance

116 We used a Seabird Electronics's SBE911+ CTD underwater unit interfaced with a sampling carousel of 24 Niskin
117 bottles, a Chelsea Acquatracka 3 fluorometer and a photosynthetically active radiation (PAR) Biospherical Licor sensor.
118 At the short stations, CTD casts were conducted at 04:00-07:00 local time (with the exception of station 1, which was
119 sampled at 08:40). At the long stations, CTD casts were conducted throughout the day but in the present report, to avoid
120 the effect of diel variability, we only consider plankton samples from the pre-dawn casts (04:00-05:00). Using CTD

casts conducted between 06:00 and 16:00, we calculated the value of the euphotic-layer vertical attenuation coefficient (k_d) after fitting the PAR data to:

$$\text{PAR}_z = \text{PAR}(0) \exp(-k_d z) \quad (1)$$

where $\text{PAR}(0)$ is the irradiance just below the surface. From this model we calculated the % PAR level for each sampling depth, which was used to determine the incubation irradiance for each sample during the primary production experiments (see section 2.5 below). We compared the daily integrated values of total solar irradiance (TSI) from the ship's pyranometer (Young 70721) and the theoretical incident PAR above the surface ($\text{PAR}(0^+)$) from the model of (Frouin et al., 1989) and used the highest ratio (corresponding to the clearest sky conditions encountered during the cruise) to obtain a conversion factor (0.42) that transforms TSI into $\text{PAR}(0^+)$. TSI units (W m^{-2}) were converted to photon flux units ($\text{mol quanta m}^{-2} \text{s}^{-1}$) by multiplying by 4.6 and a $\text{PAR}(0^-)$ to $\text{PAR}(0^+)$ ratio of 0.958 was applied (Mobley and Boss, 2012). Using k_d and $\text{PAR}(0^-)$ values for each sampling day the daily irradiance reaching each sampling depth z was calculated with Eq. 1.

2.3 Phytoplankton abundance and biomass

The abundance of phytoplankton cells with an equivalent spherical diameter (ESD) below 5-6 μm was determined with flow cytometry. Seawater samples (4.5 mL in volume) from 8-10 depths in the euphotic zone were fixed with glutaraldehyde grade I (1% final concentration), flash-frozen with liquid nitrogen and stored at -80°C until analysis. Cell counts were performed on a FACSCanto II flow cytometer (Becton Dickinson) with a flow rate of 145 $\mu\text{L min}^{-1}$ and a counting time of 5 min so that the total analysed volume for each sample was 725 μL . The separation of different autotrophic populations (*Synechococcus*, picoeukaryotes and small nanophytoplankton) was based on their scattering and fluorescence signals according to (Marie et al., 2000) and (Larsen et al., 2001). The abundance of *Prochlorococcus* was determined on 2-mL samples, also fixed with glutaraldehyde grade I (1% final concentration), and analyzed with a FACScalibur flow cytometer (Becton Dickinson) using a flow rate of 39-41 $\mu\text{L min}^{-1}$ (Zäncker et al., 2020). To obtain estimates of carbon biomass, we applied different values of cellular carbon content for each group. For *Prochlorococcus* and *Synechococcus*, we used a cell carbon content of 0.06 and 0.15 pgC cell^{-1} , respectively, which is the mean value obtained by (Buitenhuis et al., 2012) from a compilation of multiple open-ocean studies. For picoeukaryotes, we assumed a mean cell diameter of 2 μm and thus a volume of 4.2 $\mu\text{m}^3 \text{cell}^{-1}$, which gives a carbon content of 0.72 pgC cell^{-1} after applying the relationship between cell volume and cell carbon obtained by (Marañón et al., 2013) with 22 species of phytoplankton spanning 6 orders of magnitude in cell volume. For small nanophytoplankton, we assumed a mean cell diameter of 4 μm and a volume of 34 $\mu\text{m}^3 \text{cell}^{-1}$, which gives a carbon content of 4.5 pgC cell^{-1} .

The abundance of phytoplankton cells with an ESD above 5 μm was determined with an Imaging Flow CytoBot (IFCB) (Olson and Sosik, 2007), which quantitatively images chlorophyll *a*-fluorescing particles. Samples (4.7 mL) were obtained from 6-8 depths in the euphotic zone and screened through a 150- μm mesh to prevent clogging of the instrument. Size-abundance spectra obtained with microscopy image analysis in oligotrophic waters indicate that cells with a volume $\geq 10,000 \mu\text{m}^3$ (which, assuming a cylindrical, elongated shape, corresponds roughly to cells with a length of 150 μm and a diameter of 10 μm) contribute on average approximately 1% of total biovolume (Huete-Ortega et al., 2012; Marañón, 2015). It is thus unlikely that pre-screening of IFCB samples resulted in significant underestimation of total biovolume. From each obtained image, phytoplankton biovolume was computed following (Moberg and Sosik, 2012). Processed images, metadata, and derived morphometric properties were uploaded to

160 EcoTaxa (<https://ecotaxa.obs-vlfr.fr/>). The biovolume concentration was converted into a carbon biomass concentration
by applying the mean carbon to volume ratio obtained by Marañón et al. (2013) for cells larger than 5 μm in ESD (0.11
162 $\text{pgC } \mu\text{m}^{-3}$). Total phytoplankton biomass was calculated as the sum of the carbon biomass of *Prochlorococcus*,
Synechococcus, picoeukaryotes, nanoeukaryotes and $> 5 \mu\text{m}$ phytoplankton.

164 2.4 Pigments

Samples for pigment analysis with high-performance liquid chromatography (HPLC) were collected from 12 depths
166 over the 0-250 m range. Depending on particle load, a volume of 2-2.5 L of seawater was vacuum-filtered under low
pressure onto Whatman GF/F filters (ca. 0.7 μm pore size, 25 mm in diameter). The filters were flash-frozen
168 immediately after filtration in liquid nitrogen, stored at -80° during the cruise and shipped back to the laboratory in
cryo-shipping containers filled with liquid nitrogen. Filters were extracted in 3 mL of pure methanol at -20°C for one
170 hour. The extracts were vacuum-filtered through GF/F filters and then analyzed (within 24 h) by HPLC using a
complete Agilent Technologies system. The pigments were separated and quantified following the protocol described in
172 (Ras et al., 2008). Here we report the concentration of total chlorophyll *a* (TChl *a*), which includes chlorophyll *a* and
divinyl chlorophyll *a*. The fucoxanthin to TChl *a* ratio was multiplied by different factors to obtain estimates of the
174 diatom contribution to TChl *a*. The factors used were: 1.41 (Uitz et al., 2006), 1.6 (Di Cicco et al., 2017) and 1.74 (Di
Cicco, 2014). Because fucoxanthin is also present in non-diatom groups such as haptophytes and pelagophytes (Di
176 Cicco et al., 2017), which can be identified, respectively, by the marker pigments 19'-hexanoyloxyfucoxanthin (Hex-
fuco) and 19'-butanoyloxyfucoxanthin (But-fuco), we also calculated the fucoxanthin:(Hex-fuco+But-fuco) ratio.

178 2.5 Primary production

Primary production (PP) was measured with the ^{14}C -uptake technique using simulated in situ incubations on deck. For
180 each sampling depth (5-6 depths distributed between 5 m and the base of the euphotic layer), seawater was transferred
from the Niskin bottle to 4 polystyrene bottles (3 light and one dark bottles) of 70 mL in volume, which were amended
182 with 20-40 μCi of $\text{NaH}^{14}\text{CO}_3$ and incubated for 24 h in on-deck incubators that were refrigerated with running seawater
from the ship's continuous water supply. The incubators were provided with different sets of blue and neutral density
184 filters that simulated the following percentages of attenuation: 70, 52, 38, 25, 14, 7, 4, 2 and 1%. We incubated the
samples at an irradiance level (% PAR) as close as possible to the one corresponding to their depth of origin. After
186 incubation, samples were filtered, using low-pressure vacuum, through 0.2- μm polycarbonate filters (47 mm in
diameter). At 3 depths on each profile (5 m, 15-30 m and the DCM), samples were filtered sequentially through 2- μm
188 and 0.2- μm polycarbonate filters, thus allowing to determine primary production in the picophytoplankton ($< 2 \mu\text{m}$) and
the nano- plus micro-phytoplankton ($> 2 \mu\text{m}$) size classes. All filters were exposed to concentrated HCl fumes
190 overnight, to remove non-fixed, inorganic ^{14}C , and then transferred to 4-mL plastic scintillation vials to which 4 mL of
scintillation cocktail (Ultima Gold XR) were added.

192 We also measured dissolved primary production at 3 depths on each profile (surface, base of the euphotic layer and an
intermediate depth), following the method described in (Marañón et al., 2004) but using the same incubation bottles
194 employed to determine particulate primary production. Briefly, after incubation one 5-mL aliquot was taken from each
incubation bottle and filtered through a 0.2- μm polycarbonate filter (25 mm in diameter), using low-pressure vacuum.
196 Filters were processed as described above, whereas the filtrates were acidified with 100 μL of 5M HCl and maintained
in an orbital shaker for 12 hours. Then, 15 mL of liquid scintillation cocktail were added to each sample. The
198 radioactivity in all filter and filtrate samples was measured on-board with a Packard 1600TR liquid scintillation counter.

200 The percentage of extracellular release (% PER) was calculated as dissolved primary production divided by the sum of dissolved and particulate primary production.

202 To calculate daily PP, DPM counts in the dark samples were subtracted from the DPM counts in the light samples and actual values of dissolved inorganic carbon concentration, determined during the cruise at each sampling depth, were used. Given that all incubations were conducted at SST, we applied a temperature correction to the measured rates, by using the Arrhenius-van 't Hoff equation:

$$R = A e^{E_a/KT} \quad (2)$$

206 where R is the production rate, A is a coefficient, E_a is the activation energy, K is the Boltzmann's constant ($8.617 \cdot 10^{-5}$ eV $^{\circ}\text{K}^{-1}$) and T is temperature in $^{\circ}\text{K}$. The value of production rate obtained for each sampling depth incubated at SST was used to determine A, and then R was calculated for the in situ temperature at each sampling depth. Following (Wang et al., 2019), we used a value of $E_a = 0.61$ eV, which corresponds approximately to a Q_{10} value of 2.3. The turnover rate of phytoplankton biomass (growth rate, d^{-1}) was calculated by dividing the rate of production ($\text{mgC m}^{-3} \text{d}^{-1}$) by the concentration of phytoplankton carbon (mgC m^{-3}) (Kirchman, 2002).

212 2.6 Heterotrophic prokaryotic production

Heterotrophic prokaryotic production (BP) was estimated from rates of ^3H -Leucine incorporation using the microcentrifugation technique (Smith and Azam, 1992) as detailed in (Van Wambeke et al., 2020a). Briefly, triplicate 1.5-mL samples and one blank from 10 depths between surface and 250 m were incubated in the dark in two thermostated incubators set at 18.6°C for upper layers and 15.2°C for deeper layers. Leucine was added at 20 nM final concentration and the Leucine to carbon conversion factor used was $1.5 \text{ kg C mol}^{-1}$. Given that in situ temperature varied from 13.4 to 21.6°C , temperature corrections were applied by using a Q_{10} factor determined on two occasions during the cruise, when different samples were incubated simultaneously in the two incubators. We obtained two values of Q_{10} (3.9 and 3.3), from which an average value of 3.6 was used for the whole BP data set. The same Q_{10} was applied to assess the contribution of temperature to the variability of BP in the upper water column, by comparing BP at in situ temperature and at a constant temperature of 17°C .

3. Results

224 3.1 Hydrographic conditions

All three long stations were characterized by broadly similar values of sea surface temperature (SST) (20 - 21°C) and strong thermal stratification, with a 5 - 6°C thermocline extending over the 10 - 70 m depth range (Fig. 2a). Compared to TYRR, stations ION and FAST showed warmer SST and a stronger stratification, and station FAST presented the warmest subsurface waters. The depth of maximum vertical stability, as denoted by the Brunt-Väisälä frequency, took a mean value of 14 m at TYRR and 22-23 m at ION and FAST. The short stations covered a wider range of locations and consequently exhibited higher variability in SST and in the strength and vertical extent of the thermocline (Fig. S1). Throughout the cruise, nutrient concentrations were low ($< 0.5 \mu\text{mol L}^{-1}$ for nitrate and $< 0.03 \mu\text{mol L}^{-1}$ for phosphate) in the upper 50 - 60 m of the water column (Guieu et al., 2020). The nitracline, defined as the first depth where nitrate concentration exceeded $0.5 \mu\text{mol L}^{-1}$, was located at (mean \pm SD) 71 ± 3 , 105 ± 2 and 78 ± 8 m in stations TYRR, ION and FAST, respectively. The phosphacline, defined as the first depth where phosphate concentration exceeded $0.03 \mu\text{mol L}^{-1}$, was deeper: 86 ± 3 , 181 ± 7 and 90 ± 5 at TYRR, ION and FAST, respectively (Table 1). At all stations,

236 fluorescence profiles displayed a DCM (see section 3.2) which was located approximately at the 1% PAR depth and 5-
10 m above the $0.3 \text{ mol m}^{-2} \text{ d}^{-1}$ isolume (Fig. 2b, Fig. S1, Table 1). Both the DCM depth and the 1% PAR depth were
238 shallower at station TYRR (74 ± 4 and 71 ± 8 , respectively) than at station ION (96 ± 4 and 94 ± 6 , respectively), with
station FAST showing intermediate values (Fig. 2b, Table 1). The depths of both the nitracline and the phosphacline
240 were strongly correlated with the DCM depth throughout the cruise (Pearson's $r = 0.86$, $n = 23$, $p < 0.001$ for the
nitracline depth and $r = 0.74$, $n = 23$, $p < 0.001$ for the phosphacline depth).

242 3.2 Phytoplankton total chlorophyll *a*, biomass and production

Surface total chlorophyll *a* concentration (TChl *a*) was low ($\leq 0.1 \text{ mg m}^{-3}$) throughout most of the cruise (Fig. 3a,b,c;
244 Fig. S2a), with the only exception of short station 1, which sampled a filament of enhanced phytoplankton abundance
(Fig. 1). The mean surface TChl *a* was similar in all three long stations ($0.07\text{-}0.08 \text{ mg m}^{-3}$). All vertical profiles
246 displayed a marked DCM (Fig. 3a,b,c; Fig. S2a), with peak TChl *a* values in the range $0.4\text{-}0.7 \text{ mg m}^{-3}$ at stations TYRR
and ION and $0.4\text{-}1.0 \text{ mg m}^{-3}$ at station FAST. The mean DCM TChl *a* at the three stations was similar (0.6 mg m^{-3})
248 (Table 1). Vertically integrated (from surface to the euphotic layer depth) TChl *a* was higher and more variable at FAST
($21 \pm 9 \text{ mg m}^{-2}$) compared with TYRR ($16 \pm 2 \text{ mg m}^{-2}$) and ION ($18 \pm 2 \text{ mg m}^{-2}$) (Table 1).

250 Phytoplankton carbon biomass tended to increase with depth, exhibiting maxima at either intermediate depths (40-50
m) or at the base of the euphotic layer (80-100 m) (Fig. 3d,e,f; Fig. S2b). The concentration of phytoplankton C in
252 surface waters was relatively invariant at 6 mgC m^{-3} whereas mean biomass values at the DCM in stations TYRR, ION
and FAST were 135 ± 8 , 144 ± 1 and $16 \pm 10 \text{ mgC m}^{-3}$, respectively (Table 1). Thus the increase, from the surface to
254 the base of the euphotic layer, in phytoplankton biomass was ca. 2.5-fold, compared with ca. 8-fold for TChl *a*.
Comparing the mean deep to surface ratios in TChl *a* and C biomass in the three stations indicates that increased
256 phytoplankton biomass was responsible for 229-341 % of the increased TChl *a* at the DCM, while photoacclimation
(decreased C:Chl *a* at depth) was responsible for the remaining 6659-718 %.

258 Compared to surface values, the deep maxima in phytoplankton C biomass were of smaller magnitude than those of
TChl *a*. Consequently, the mean C:Chl *a* ratio (g:g) was much higher at the surface (89-97) than at the DCM (21-34) at
260 all long stations (Table 1). Considering together the data from all stations, C:Chl *a* increased with light availability
following a saturating curve (Fig. 4a). Particulate primary production (PP) ranged between 1 and $3 \text{ mgC m}^{-3} \text{ d}^{-1}$ in
262 surface waters, and tended to increase with depth (Fig. 3h,i,j; Fig. S2c). In most profiles (19 out of 23), the highest
value of PP (typically, $3\text{-}6 \text{ mgC m}^{-3} \text{ d}^{-1}$) was measured in the deepest sample, corresponding to the DCM. There were
264 only small differences in mean integrated PP among stations, which ranged between 170 ± 36 and $209 \pm 67 \text{ mgC m}^{-2} \text{ d}^{-1}$
at TYRR and FAST, respectively (Table 1).

266 The contribution of cells larger than $52 \mu\text{m}$ in diameter (~~nano and micro phytoplankton~~) to total phytoplankton biomass
increased slightly with depth ~~from ca. 60% at the surface to ca. 80% at the base of the euphotic layer, and took taking~~
268 an overall mean value of 6849 ± 134 % for all samples pooled together (Fig. S3a). The contribution of the $> 2 \mu\text{m}$ size
class to total PP was relatively stable both among stations and with depth, taking a mean value of 73 ± 6 % in the long
270 stations (Fig. S3b). In contrast, the percentage of extracellular release (PER) showed a marked vertical pattern in all
stations, decreasing with depth from a mean value of 42 ± 8 % at the surface to 22 ± 4 % at the DCM (Fig. S3c).

272 TChl *a*-specific primary production (P^{Chl}) displayed a marked light dependence, following a saturating function of light
availability and reaching values of $20\text{-}35 \text{ mgC mgChl } a^{-1} \text{ d}^{-1}$ at near-surface irradiance levels (Fig. 4b). In contrast, the
274 ratio between primary production and phytoplankton C biomass (P^{C} , equivalent to a biomass turnover rate) was

independent of irradiance (Pearson's $r = 0.17$, $n = 77$, $p = 0.14$), with most values falling within the range 0.1-0.5 d⁻¹ throughout the euphotic layer (Fig. 4c). Overall, the mean P^C for the whole cruise was 0.3 ± 0.1 d⁻¹ and the same mean P^C (0.3 d⁻¹) was measured in the surface and the DCM.

3.3 ~~Fucoxanthin to total chlorophyll *a*~~ Vertical distribution of pigment ratios

The fucoxanthin to total chlorophyll *a* ratio (Fuco:TChl *a*) consistently increased below the upper 40-50 m in all long stations (Fig. 5). Fuco:TChl *a* mean values at the surface were 0.036 ± 0.001 at TYRR, 0.040 ± 0.004 at ION and 0.051 ± 0.005 at FAST (Table 1). Using different conversion factors (see Methods), these ratios translate into a range of diatom contribution to TChl *a* of 5-6 %, 6-7 % and 7-9 % at TYRR, ION and FAST, respectively. At the DCM, Fuco:TChl *a* was 0.21 ± 0.04 at TYRR, 0.29 ± 0.03 at ION and 0.24 ± 0.10 at FAST, which corresponds to diatom contributions of 30-36 %, 41-51 % and 34-42 %, respectively. The vertical distribution of the fucoxanthin:(19' hex-fuco+19' but-fuco) ratio also showed a marked increase below 40-50 m in all stations (Fig. S4), which means that the high values of the Fuco:TChl *a* ratio at depth reflect an increased contribution of diatoms. This was confirmed by the images obtained with the IFCB, which show that diatoms were abundant at the DCM in all three long stations whereas they were virtually absent in the surface samples (Fig. S5).

3.4 Heterotrophic prokaryotic production and relationship with primary production

Rates of heterotrophic prokaryotic production (BP) in the euphotic layer fell within the range 10-50 ngC L⁻¹ h⁻¹ and took values < 10 ngC L⁻¹ h⁻¹ in the waters below (Fig. 6, Fig. S64). Most vertical profiles of BP were characterized by two peaks: one at the surface and another one in sub-surface waters, coinciding with the DCM or slightly above it. We assessed the effect of temperature on BP rates in the upper layer (0-50 m) by comparing the rates calculated at in situ temperature versus a constant temperature of 17°C (mean temperature for all profiles across 0-250 m). While BP rates at in situ temperature displayed a marked increase in the 2-3 most shallow sampling depths, BP at a constant temperature of 17°C remained largely homogenous with depth (Fig. S75). The mean integrated BP at the long stations ranged between 50-60 mgC m⁻² d⁻¹ in stations TYRR and ION and ca. 90 mgC m⁻² d⁻¹ in station FAST (Table 1). Considering all data in the euphotic layer, there was a positive correlation between both particulate and dissolved primary production and BP (Fig. 7). However, primary production explained less than 10% of the variability in BP. Taking into account that BP displayed a surface maximum, which was rarely observed in the primary production profiles, we explored the relationship between PP and BP in samples from below 30 m (Fig. S86). Although a positive relationship was observed, PP still explained only a small amount of variability in BP, which reflects the fact that the deep maximum in BP was often shallower than the deep PP maximum.

4. Discussion

4.1 Seasonal and geographical context

The vertical location and longitudinal variability of the DCM we observed agree with the patterns previously reported for the Mediterranean Sea, based both on climatological analyses of chlorophyll *a* profiles (Lavigne et al., 2015) and time-series studies (Lemée et al., 2002; Marty et al., 2002). In the western basin, where the spring bloom is characterized by the presence of a surface chlorophyll maximum, a subsurface maximum develops from April onwards that takes progressively a deeper location, reaching 70-80 m in mid-summer. This deepening of the DCM occurs later in the north than in the south section of the western basin (Lavigne et al., 2015). In agreement, we found during PEACETIME that the stations located in the southwest had deeper DCMs than those located in the northwest (it has to

314 be noted, though, that the seasonal evolution during the cruise may have influenced the DCM depth and that the southwestern stations were sampled last). In the central Mediterranean (e.g. Ionian Sea), the spring surface chlorophyll maximum does not occur, and the DCM also appears around April but becomes deeper than in the western region. 316 Accordingly, during our cruise the DCM at long station ION was significantly deeper than at the western stations. We also found, as previously described in analyses of vertical structure in stratified waters (Herbland and Voituriez, 1979; 318 Letelier et al., 2004; Cullen, 2015), a general correspondence between the top of the nutricline and the depth of the DCM, with deeper values in the Ionian Sea than in the western basin. These differences reflect the more persistent stratification and stronger degree of oligotrophy that characterizes the central and eastern basins as compared to the 320 western Mediterranean Sea (Bosc et al., 2004; D'Ortenzio and Ribera d'Alcalà, 2009). The nitracline was deeper than the DCM at ION, which reflects longitudinal differences in the way the DCM and the mixed layer depth are coupled in the Mediterranean Sea, as described by Barbieux et al. (2019). These authors concluded that in the Ionian and Levantine basins the deepest winter mixed layer rarely reaches the top of the nutricline and the DCM is persistently well above the nutricline during the stratified season. 322 324

326 Numerous surveys at fixed stations (Lemée et al., 2002; Marty and Chiavérini, 2002) as well as along oceanographic transects (Estrada, 1996; Moutin and Raimbault, 2002; López-Sandoval et al., 2011) have described the vertical 328 variability of PP in the Mediterranean Sea during the stratification season. While subsurface maxima are often observed in late spring and summer, these peaks tend to be located above rather than at the DCM (Estrada, 1996; Marty and Chiavérini, 2002). During the MINOS cruise, which sampled the entire Mediterranean Sea from the western to the 330 Levantine basin in May-June 1996, (Moutin and Raimbault, 2002) found a strong correlation between the depths of the deep PP peak and the DCM depth, but the former was on average 20 m shallower. In contrast, during PEACETIME the mean depths of the primary production maximum and the DCM coincided and only on 3 profiles was the primary 332 production peak located above the DCM. One potential source of bias during our ¹⁴C-uptake experiments could come from the fact that all samples were incubated at sea surface temperature. However, the correction we applied to the 334 measured rates assumes a relatively strong degree of temperature dependence (an activation energy of 0.66 eV), while oligotrophic conditions, prevailing during the cruise, are known to result in decreased temperature sensitivity of 336 phytoplankton metabolic rates (O'Connor et al., 2009; Marañón et al., 2018). Had we used a lower temperature sensitivity in our corrections, the magnitude of the deep production peaks would have been even greater. Thanks to the 338 combined measurements of cell abundance and biovolume together with photosynthetic carbon fixation, it is possible to explore the variability in phytoplankton biomass and its turnover rate, to assess if the measured deep production peaks 340 are plausible and explore which processes may have been responsible for their occurrence (section 4.2). 342

Our estimates of growth rate also allowed us to assess if phytoplankton inhabiting the surface waters of the 344 Mediterranean Sea during the stratification season were just experiencing nutrient limitation of their standing stock (yield limitation sensu Liebig) or if they are also limited in their rate of resource use (physiological rate limitation sensu Blackman). As demonstrated in chemostat experiments (Goldman et al., 1979), fast growth rates are compatible with 346 extremely low ambient nutrient concentrations and therefore oligotrophy in itself does not necessarily imply that Blackman limitation is operating. However, the mean growth rate measured in surface waters during the PEACETIME 348 cruise (0.3 d^{-1}) is well below the maximal, nutrient-saturated growth rate that could be expected at warm ($> 20^\circ\text{C}$) temperatures for different groups such as diatoms, cyanobacteria and green algae ($\geq 1 \text{ d}^{-1}$) (Kremer et al., 2017). 350 Similarly low ($0.2\text{-}0.6 \text{ d}^{-1}$) phytoplankton growth rates have been reported before for the western Mediterranean Sea (Pedrós-Alió et al., 1999) and oligotrophic regions of the Atlantic subtropical gyres (Marañón, 2005; Armengol et al., 352 2019) and the North Pacific (Landry et al., 2008; Landry et al., 2009; Berthelot et al., 2019). Multiple experimental

354 approaches, including in situ iron additions (Boyd et al., 2007; Yoon et al., 2018) in high-nutrient, low-chlorophyll
regions as well as in vitro bioassays with inorganic nutrients (Mills et al., 2004; Tanaka et al., 2011; Tsiola et al., 2016)
356 and desert dust (Marañón et al., 2010; Guieu et al., 2014) in low-nutrient, low-chlorophyll regions, typically display
larger increases in carbon fixation and nutrient uptake rates than in photoautotroph abundance, which implies enhanced
358 biomass turnover rates upon alleviation of nutrient scarcity. Therefore low nutrient availability, which is widespread in
the global ocean (Moore et al., 2013), results not only in low phytoplankton biomass but also in slow growth rates.

360 **4.2 Mechanisms underlying deep production maxima**

Earlier studies have shown that both photoacclimation and enhanced biomass contribute to the occurrence of the DCM
362 in the western Mediterranean Sea whereas in the central and eastern basins photoacclimation alone would be mainly
responsible for the increased chlorophyll *a* at depth (Estrada, 1996; Mignot et al., 2014; Barbieux et al., 2019). In
364 contrast, during our survey the contribution of increased phytoplankton biomass was similar in all stations, including
the one located in the Ionian Sea. Most (ca. 75%) of the increased Chl *a* concentration at the DCM at all stations was
366 due to photoacclimation, the rest being a result of increased biomass. The C:Chl *a* ratios (g:g) we estimate
(approximately 90-100 and 20-30 for surface and DCM populations, respectively) agree well with previous results from
368 the Mediterranean Sea (Estrada, 1996) and the Atlantic subtropical gyres (Veldhuis and Kraay, 2004; Marañón, 2005;
Pérez et al., 2006) as well as with general patterns observed in light- and nutrient-limited laboratory cultures (MacIntyre
370 et al., 2002; Halsey and Jones, 2015; Behrenfeld et al., 2016). The fact that high C:Chl *a* values (> 50) persisted
throughout the water column until PAR was lower than 2 mol m⁻² d⁻¹ suggests that nutrient limitation prevailed over
372 most of the euphotic layer, because under nutrient-sufficient and light-limited conditions C:Chl *a* typically takes values
< 30 (Halsey and Jones, 2015). Only the populations inhabiting the DCM showed clear signs of light limitation,
374 reflected in the decreased C:Chl *a* ratios. The question remains whether those populations were mainly sustained by
new nutrients supplied by diffusion from below the nutricline or by recycled nutrients originated within the euphotic
376 layer.

(Taillandier et al., 2020) combined measurements of the vertical gradient in nutrient concentrations during
378 PEACETIME with estimates of diffusivity based on turbulent kinetic energy dissipation rates measured by (Ferron et
al., 2017) in the western Mediterranean Sea, which allowed them to calculate the vertical diffusive fluxes across the
380 nutricline in the Tyrrhenian Sea and the Algerian Basin. We used these fluxes to estimate the contribution of new
nutrients to sustain phytoplankton productivity at the deep biomass maximum in stations TYRR and FAST, given the
382 observed biomass concentration and turnover rate (Table 2) and assuming that the deep biomass maximum extended
over 30 m. These calculations suggest that diffusive fluxes could provide only a small fraction of the nitrogen and,
384 especially, the phosphorus requirements of the phytoplankton assemblages inhabiting the lower part of the euphotic
layer. Thus most of the primary production in the euphotic layer was sustained by recycled nutrients, which agrees with
386 the observation that phytoplankton growth rates did not show any increase at the DCM despite the proximity of the
nutricline. The broadly homogeneous distribution of phytoplankton growth throughout the euphotic layer also supports
388 the conclusion of (Fennel and Boss, 2003) that deep phytoplankton maxima develop approximately at the compensation
depth, where growth and losses balance each other. We can speculate that the compensation depth during our cruise
390 broadly coincided with the 1% PAR light level or 0.5 mol m⁻² d⁻¹ isolume but additional primary production
measurements in deeper samples would have been required to test this hypothesis.

392 The nano- and micro-phytoplankton size classes consistently dominated primary production during the cruise,
accounting on average for ca. 70% of total carbon fixation. The relatively low share (\leq 30-35 %) of primary production

394 due to picophytoplankton agrees well with previous results based on remote sensing across the entire Mediterranean Sea
(Uitz et al., 2012) while field measurements conducted in the western and central basins during the stratification season
396 show somewhat higher and more variable picophytoplankton contribution (Magazzù and Decembrini, 1995;
Decembrini et al., 2009). During PEACETIME, ~~the contribution of cells > 5 µm in diameter to total phytoplankton~~
398 ~~biomass increased with depth, and this trend was associated with a~~ there a was significant increase with depth in the
contribution of diatoms to total phytoplankton biomass, which reached at least 30 % in the DCM of all stations, and was
400 particularly high (nearly 50 %) in the most stratified station, located in the Ionian Sea. Deep maxima in diatom
abundance are common in the Mediterranean Sea during stratified conditions (Ignatiades et al., 2009; Siokou-Frangou
402 et al., 2010; Mena et al., 2019) and are often associated with peaks in biogenic silica (Crombet et al., 2011). The
increased prevalence of diatoms at the base of the euphotic layer, which illustrates the ecological diversity of this group
404 (Kemp and Villareal, 2018), is likely a result of multiple adaptations and mechanisms, including high growth efficiency
under low light conditions (Fisher and Halsey, 2016), buoyancy regulation (Villareal et al., 1996), the ability to exploit
406 transient nutrient pulses through luxury uptake and storage (Cermeño et al., 2011; Kemp and Villareal, 2013) and the
enhanced ammonium assimilation mediated by microbial interactions in the phycosphere (Olofsson et al., 2019).
408 However, our observations were restricted in time and therefore it remains uncertain whether the important presence of
diatoms in the DCM observed during our cruise persists during the whole stratification season or if it was associated
410 with the downward export from the previous spring bloom, as previously observed in the western Mediterranean Sea
(Estrada et al., 1993).

412 4.3 Phytoplankton photophysiology and productivity

Although the widespread occurrence of deep chlorophyll maxima, which cannot be detected by ocean colour sensors, is
414 often mentioned as a shortcoming of satellite-based productivity models, the vertical distribution of chlorophyll *a*
concentration can be derived from surface optical properties (Morel and Berthon, 1989; Uitz et al., 2006). The key
416 challenge rests in the quantification of the photophysiological parameters (e.g. photosynthetic efficiency), required to
convert photoautotroph biomass or pigment concentration into a measure of carbon fixation. Of especial relevance, in
418 the case of low-light acclimated populations, is the initial slope in the relationship between irradiance and Chl *a*-specific
photosynthesis (α^B , $\text{mgC (mgChl } a)^{-1} \text{ h}^{-1}$ ($\mu\text{mol photon m}^{-2} \text{ s}^{-1}$) $^{-1}$). Using a large dataset of photosynthetic parameters
420 obtained with the same method, (Uitz et al., 2008) found that α^B took a mean value of 0.025 ± 0.022 in the lower part of
the euphotic layer in oligotrophic regions across the world's oceans. Assuming 14 h of daylight and that night-time
422 respiration losses account for 20 % of carbon fixed during the day (Geider, 1992), and given the mean Chl *a*
concentration (0.6 mg m^{-3}) and daily PAR ($0.5 \text{ mol m}^{-2} \text{ d}^{-1}$) measured at the DCM during PEACETIME, this value of
424 α^B translates into a primary production $< 1.7 \text{ mgC m}^{-3} \text{ d}^{-1}$, lower than the rates we measured ($2\text{-}10 \text{ mgC m}^{-3} \text{ d}^{-1}$).
Interestingly, the mean α^B value determined at the base of the euphotic layer during the PROSOPE cruise, which
426 sampled all major basins of the Mediterranean Sea in September 1999, was 0.066 ± 0.024 , which would correspond to a
DCM primary production of $4.4 \text{ mg C m}^{-3} \text{ d}^{-1}$, in agreement with our observations. The low α^B value reported by Uitz et
428 al. (2008) largely reflected the photophysiological properties of communities dominated by small cells, in contrast with
the assemblages encountered during the present study. It thus would appear that the high primary production at the
430 DCM during PEACETIME was due not only to enhanced levels of phytoplankton biomass but also to the presence of a
diatom-rich community characterised by high photosynthetic efficiency. These results stress the importance of
432 incorporating the linkage between community structure and photophysiological parameters to improve the application
of bio-optical productivity models over diverse ecological and biogeographic settings (Uitz et al., 2010; Uitz et al.,
434 2012; Robinson et al., 2018).

We found that phytoplankton can sustain similar rates of biomass-specific carbon fixation across a wide range of irradiances, in spite of considerable variations in Chl *a*-specific photosynthesis. The uncoupling between these two metrics of productivity likely arises from photoacclimation, whereby cells receiving less irradiance invest more resources in light-harvesting complexes and are thus capable of sustaining similar rates of nutrient-limited carbon fixation (per unit biomass) as cells experiencing high light availability (Pan et al., 1996). Using a photoacclimation model in conjunction with satellite observations of phytoplankton carbon and Chl *a*, (Behrenfeld et al., 2016) demonstrated that most of the seasonal and interannual variability in surface Chl *a* concentration of multiple ocean biomes resulted from photoacclimation and therefore cannot be readily translated into equivalent changes in productivity. Our results suggest that the same conclusion also applies to small-scale vertical variability in stratified environments, where phytoplankton growth rates are often relatively constant across the euphotic layer (Pérez et al., 2006; Cáceres et al., 2013; Armengol et al., 2019; Berthelot et al., 2019). ~~More generally, t~~The fact that C:Chl *a* is highly sensitive not only to irradiance but to nutrient availability and temperature as well (Geider, 1987; Halsey and Jones, 2015) means that changes in growth rate can be disconnected from Chl *a*-specific photosynthesis across multiple environmental gradients (Cullen et al., 1992; Marañón et al., 2018). The apparent paradox of constant phytoplankton growth rates across the euphotic layer, in spite of marked changes in both temperature and light availability, can be explained by considering that the physiological effect of a given environmental factor tends to decrease when another factor is limiting (Cross et al., 2015; Edwards et al., 2016; Marañón et al., 2018). Thus the lack of irradiance effects on the growth rate of acclimated phytoplankton assemblages may have resulted from the fact that nutrient limitation prevailed throughout the water column.

4.4 Relationship between heterotrophic prokaryotic and primary production

The vertical distribution of BP, which was characterized by the presence of both surface and deep maxima, likely reflects the combined influence of several controlling factors. Different studies have investigated the relationship between temperature, inorganic nutrients and dissolved organic matter availability as drivers of heterotrophic prokaryotic production and carbon demand in the Mediterranean Sea over seasonal (Lemée et al., 2002; Alonso-Sáez et al., 2008; Cúa et al., 2015) and mesoscale to basin-scale (Pedrós-Alió et al., 1999; Pulido-Villena et al., 2012) ranges of variability but the relative role of these factors at the small vertical scale within the upper water column has been comparatively less explored. (Van Wambeke et al., 2002) reported that BP consistently peaked at the surface during a mesoscale survey in the Gulf of Lions in spring, which was probably a result of the fact that primary production also increased in the surface layer, a pattern also reported by (Lemée et al., 2002) throughout most of the year in the DYFAMED station. In the case of the PEACETIME cruise, however, the surface peak in BP cannot be attributed to increased primary production, which took the lowest values in the surface layer. Temperature, which exhibited a ca. 5°C-gradient over the upper 50 m, appears as the most likely responsible driver of the surface BP peaks, considering that the estimated rates at a constant temperature of 17°C were nearly homogeneous across the upper layer. Seasonal studies in coastal waters of the western Mediterranean Sea have also identified temperature as a factor that contributes to explain the temporal variability of bacterial production in surface waters (Alonso-Sáez et al., 2008; Cúa et al., 2015). In contrast, the deep peak in BP found during our cruise was associated, at least in part, with increased phytoplankton biomass and production, so an enhanced availability of organic substrates may have been responsible for the stimulation of bacterial activity near the base of the euphotic layer.

Atmospheric deposition of nutrients may have also contributed to sustain the surface BP peaks observed during our study. Nitrogen and phosphorus amendments to seawater from the mixed layer resulted in BP stimulation after 48 h, indicating NP co-limitation of BP, whereas addition of a labile carbon source (glucose) had no effect (Van Wambeke et

476 al., 2020b). Thus the surface BP peak observed under in situ conditions was not due to dependence of organic carbon
477 substrates but may have resulted in part from new N and P availability through dry atmospheric deposition. The
478 superior ability of heterotrophic bacteria to compete for inorganic nutrients has been shown by the budget analysis and
479 experimental observations of (Van Wambeke et al., 2020b), who concluded that dry atmospheric deposition could
480 supply nearly 40% of the heterotrophic bacteria N demand in the upper mixed layer during the stratification season in the
481 Mediterranean Sea.

482 ~~The same study shows that atmospheric dry deposition during the PEACETIME cruise could sustain about 13% of the~~
483 ~~heterotrophic bacterial N demand within the mixed layer. Other sources of N fueling heterotrophic bacteria could come~~
484 ~~from recycling, as for instance hydrolysis of proteins satisfied a mean of 47% of that demand (Van Wambeke et al.,~~
485 ~~2020).~~

486 Despite the association between increased PP and increased BP in subsurface waters, the overall strength of the
487 relationship between these two variables during PEACETIME was weak. This in contrast with previous analyses in the
488 Mediterranean Sea that included a much broader range of plankton biomass and production regimes than the one
489 covered during our cruise and found stronger correlations between photosynthetic carbon fixation and BP (Turley et al.,
490 2000; Pulido-Villena et al., 2012). If we consider the trophic coupling between heterotrophic bacteria and
491 phytoplankton as the extent to which dissolved primary production meets heterotrophic bacterial carbon demand
492 (Morán et al., 2002), our results suggest a poor coupling during the PEACETIME cruise. Assuming a value of bacterial
493 growth efficiency of 10 %, as determined in the western Mediterranean Sea during summer (Lemée et al., 2002;
494 Alonso-Sáez et al., 2008), our measured rates of dissolved primary production represented, on average, only 25 % (SD
495 = 14 %) of estimated bacterial carbon demand. Similar weak phytoplankton-bacterioplankton coupling has been
496 reported before for the Mediterranean Sea during the stratification period (Morán et al., 2002; Alonso-Sáez et al., 2008;
497 López-Sandoval et al., 2011), which emphasizes the role of additional substrates, other than recent products of
498 photosynthesis released in dissolved form, in fuelling bacterial metabolism. These additional substrates can include
499 dissolved organic carbon released by consumers (e.g. sloppy feeding) or during cell lysis, as well as organic molecules
500 previously produced and accumulated over time scales longer than 1 day or derived from allochthonous sources such as
501 river and atmospheric inputs. However, the fact that bacterial carbon demand often exceeds the instantaneous rate of
502 dissolved primary production does not mean that bacterial metabolism is independent of phytoplankton photosynthesis
503 over annual scales, but rather reflects the temporal uncoupling resulting from the episodic nature of phytoplankton
504 production events (Steinberg et al., 2001; Karl et al., 2003; Morán and Alonso-Sáez, 2011).

4.5 Conclusions

506 We have shown that the DCM in the western Mediterranean Sea during the stratification period, already known to be a
507 phytoplankton biomass maximum, can also represent a substantial primary production maximum. These deep maxima
508 in biomass and primary production are not associated with an increase in phytoplankton growth rates and do not seem to
509 be fueled by new nutrients, but likely arise as a result of cell sinking from above in combination with the high
510 photosynthetic efficiency of a diatom-rich, low-light acclimated community, which sustains similar growth rates as
511 those measured in the upper, well-illuminated layers. Because of the variability in C:Chl *a* ratios, changes in Chl *a*-
512 specific primary production can be disconnected from biomass turnover rates. While the trophic coupling between
513 heterotrophic bacteria and phytoplankton was relatively poor, the increased photosynthetic biomass and carbon fixation
514 measured near the base of the euphotic zone did result in an enhancement of bacterial heterotrophic activity, which in
the surface layers appeared to be regulated by temperature. Our results support the combined use of isotope uptake

516 measurements and biovolume-based estimates of phytoplankton carbon biomass to derive growth rates at discrete
depths and gain insight into the mechanisms underlying the DCM. Data with higher spatial and temporal resolution, as
518 derived for instance from optical sensors attached to autonomous instruments, will allow to establish if the marked
peaks in primary production we observed are a persistent feature of the DCM in the central and western Mediterranean
520 Sea, and to quantify their broader biogeochemical significance.

Data availability

522 All data from the PEACETIME cruise (<https://doi.org/10.17600/17000300>) are stored at the LEFE CYBER Database
(<http://www.obs-vlfr.fr/proof/php/PEACETIME/peacetime.php>) and will be made freely available once all manuscripts
524 are submitted to the PEACETIME special issue. In the meantime, data can be also obtained upon request to the **first**
corresponding author.

Acknowledgements

This study is a contribution to the PEACETIME project (<http://peacetime-project.org>), a joint initiative of the
528 MERMEX and ChArMEx components supported by CNRS-INSU, IFREMER, CEA, and Météo-France as part of the
programme MISTRALS coordinated by INSU. The research of EM and MPL was funded by the Spanish Ministry of
530 Science, Innovation and Universities through grant PGC2018-094553B-I00 (POLARIS) and by the European Union
through H2020 project ‘Tropical and South Atlantic climate-based marine ecosystem predictions for sustainable
532 management’ (TRIATLAS, Grant agreement No 817578). We acknowledge the French Centre National d’Etudes
Spatiales (CNES), which supported the bio-optical and ocean color component of the PEACETIME project
534 (PEACETIME-OC). We also thank the *Service d’analyse de pigments par HPLC* (SAPIGH) at the Institut de la Mer de
Villefranche (IMEV) for HPLC analysis, as well as the captain and crew of the R/V *Pourquoi Pas?* for their help during
536 the work at sea.

References

- 538 Alonso-Sáez, L., Vázquez-Domínguez, E., Cardelús, C., Pinhassi, J., Sala, M. M., Lekunberri, I., Balagué, V., Vila-
Costa, M., Unrein, F., Massana, R., Simó, R., and Gasol, J. M.: Factors Controlling the Year-Round Variability in
540 Carbon Flux Through Bacteria in a Coastal Marine System, *Ecosystems*, 11, 397-409, 10.1007/s10021-008-9129-0,
2008.
- 542 Antoine, D., Morel, A., and André, J.-M.: Algal pigment distribution and primary production in the eastern
Mediterranean as derived from coastal zone color scanner observations, *Journal of Geophysical Research: Oceans*, 100,
544 16193-16209, 10.1029/95jc00466, 1995.
- Armengol, L., Calbet, A., Franchy, G., Rodríguez-Santos, A., and Hernández-León, S.: Planktonic food web structure
546 and trophic transfer efficiency along a productivity gradient in the tropical and subtropical Atlantic Ocean, *Scientific*
Reports, 9, 2044, 10.1038/s41598-019-38507-9, 2019.
- 548 Barbieux, M., Uitz, J., Gentili, B., Pasquero de Fommervault, O., Mignot, A., Poteau, A., Schmechtig, C., Taillandier,
V., Leymarie, E., Penkerch, C., D’Ortenzio, F., Claustre, H., and Bricaud, A.: Bio-optical characterization of subsurface
550 chlorophyll maxima in the Mediterranean Sea from a Biogeochemical-Argo float database, *Biogeosciences*, 16, 1321-
1342, 10.5194/bg-16-1321-2019, 2019.
- 552 Beckmann, A., and Hense, I.: Beneath the surface: Characteristics of oceanic ecosystems under weak mixing conditions
– A theoretical investigation, *Progress in Oceanography*, 75, 771-796, <https://doi.org/10.1016/j.pocean.2007.09.002>,
554 2007.
- 556 Behrenfeld, M. J., O’Malley, R. T., Boss, E. S., Westberry, T. K., Graff, J. R., Halsey, K. H., Milligan, A. J., Siegel, D.
A., and Brown, M. B.: Revaluating ocean warming impacts on global phytoplankton, *Nature Climate Change*, 6, 323-
330, 10.1038/nclimate2838, 2016.

- 558 Berthelot, H., Duhamel, S., L'Helguen, S., Maguer, J. F., Wang, S., Cetinić, I., and Cassar, N.: NanoSIMS single cell
560 analyses reveal the contrasting nitrogen sources for small phytoplankton, *ISME J*, 13, 651-662, 10.1038/s41396-018-
0285-8, 2019.
- Bosc, E., Bricaud, A., and Antoine, D.: Seasonal and interannual variability in algal biomass and primary production in
562 the Mediterranean Sea, as derived from 4 years of SeaWiFS observations, *Global Biogeochemical Cycles*, 18,
10.1029/2003gb002034, 2004.
- 564 Boyd, P. W., Jickells, T., Law, C. S., Blain, S., Boyle, E. A., Buesseler, K. O., Coale, K. H., Cullen, J. J., de Baar, H. J.
566 W., Follows, M., Harvey, M., Lancelot, C., Levasseur, M., Owens, N. P. J., Pollard, R., Rivkin, R. B., Sarmiento, J.,
Schoemann, V., Smetacek, V., Takeda, S., Tsuda, A., Turner, S., and Watson, A. J.: Mesoscale Iron Enrichment
Experiments 1993-2005: Synthesis and Future Directions, *Science*, 315, 612-617, 10.1126/science.1131669, 2007.
- 568 Buitenhuis, E. T., Li, W. K. W., Vaultot, D., Lomas, M. W., Landry, M. R., Partensky, F., Karl, D. M., Ulloa, O.,
570 Campbell, L., Jacquet, S., Lantoin, F., Chavez, F., Macias, D., Gosselin, M., and McManus, G. B.: Picophytoplankton
biomass distribution in the global ocean, *Earth Syst. Sci. Data*, 4, 37-46, 10.5194/essd-4-37-2012, 2012.
- Cáceres, C., Taboada, F. G., Höfer, J., and Anadón, R.: Phytoplankton Growth and Microzooplankton Grazing in the
572 Subtropical Northeast Atlantic, *PLOS ONE*, 8, e69159, 10.1371/journal.pone.0069159, 2013.
- Céa, B., Lefèvre, D., Chirurgien, L., Raimbault, P., Garcia, N., Charrière, B., Grégori, G., Ghiglione, J. F., Barani, A.,
574 Lafont, M., and Van Wambeke, F.: An annual survey of bacterial production, respiration and ectoenzyme activity in
coastal NW Mediterranean waters: temperature and resource controls, *Environmental Science and Pollution Research*,
576 22, 13654-13668, 10.1007/s11356-014-3500-9, 2015.
- Cermeño, P., Lee, J. B., Wyman, K., Schofield, O., and Falkowski, P. G.: Competitive dynamics in two species of
578 marine phytoplankton under non-equilibrium conditions, *Marine Ecology Progress Series*, 429, 19-28, 2011.
- Claustre, H., Morel, A., Babin, M., Cailliau, C., Marie, D., Marty, J.-C., Tailliez, D., and Vaultot, D.: Variability in
580 particle attenuation and chlorophyll fluorescence in the tropical Pacific: Scales, patterns, and biogeochemical
implications, *Journal of Geophysical Research: Oceans*, 104, 3401-3422, 10.1029/98jc01334, 1999.
- 582 Crombet, Y., Leblanc, K., Quéguiner, B., Moutin, T., Rimmelin, P., Ras, J., Claustre, H., Leblond, N., Oriol, L., and
584 Pujo-Pay, M.: Deep silicon maxima in the stratified oligotrophic Mediterranean Sea, *Biogeosciences*, 8, 459-475,
10.5194/bg-8-459-2011, 2011.
- Cross, W. F., Hood, J. M., Benstead, J. P., Huryn, A. D., and Nelson, D.: Interactions between temperature and nutrients
586 across levels of ecological organization, *Global Change Biology*, 21, 1025-1040, <https://doi.org/10.1111/gcb.12809>,
2015.
- 588 Cullen, J. J., Yang, X., and MacIntyre, H. L.: Nutrient Limitation of Marine Photosynthesis, in: *Primary Productivity
590 and Biogeochemical Cycles in the Sea*, edited by: Falkowski, P. G., Woodhead, A. D., and Vivirito, K., Springer US,
Boston, MA, 69-88, 1992.
- Cullen, J. J.: Subsurface Chlorophyll Maximum Layers: Enduring Enigma or Mystery Solved?, *Annual Review of
592 Marine Science*, 7, 207-239, 10.1146/annurev-marine-010213-135111, 2015.
- D'Ortenzio, F., and Ribera d'Alcalà, M.: On the trophic regimes of the Mediterranean Sea: a satellite analysis,
594 *Biogeosciences*, 6, 139-148, 10.5194/bg-6-139-2009, 2009.
- Decembrini, F., Caroppo, C., and Azzaro, M.: Size structure and production of phytoplankton community and carbon
596 pathways channelling in the Southern Tyrrhenian Sea (Western Mediterranean), *Deep Sea Research Part II: Topical
Studies in Oceanography*, 56, 687-699, <https://doi.org/10.1016/j.dsr2.2008.07.022>, 2009.
- 598 Di Cicco, A.: *Spatial and Temporal Variability of Dominant Phytoplankton Size Classes in the Mediterranean Sea from
Remote Sensing*, PhD, Tuscia University, 2014.
- 600 Di Cicco, A., Sammartino, M., Marullo, S., and Santoleri, R.: Regional Empirical Algorithms for an Improved
602 Identification of Phytoplankton Functional Types and Size Classes in the Mediterranean Sea Using Satellite Data,
Frontiers in Marine Science, 4, 10.3389/fmars.2017.00126, 2017.

- 604 Durham, W. M., and Stocker, R.: Thin Phytoplankton Layers: Characteristics, Mechanisms, and Consequences, *Annual Review of Marine Science*, 4, 177-207, 10.1146/annurev-marine-120710-100957, 2012.
- 606 Edwards, K. F., Thomas, M. K., Klausmeier, C. A., and Litchman, E.: Phytoplankton growth and the interaction of light and temperature: A synthesis at the species and community level, *Limnology and Oceanography*, 61, 1232-1244, <https://doi.org/10.1002/lno.10282>, 2016.
- 608 Estrada, M., Marrasé, C., Latasa, M., Berdalet, E., Delgado, M., and Riera, T.: Variability of deep chlorophyll maximum characteristics in the Northwestern Mediterranean, *Marine Ecology Progress Series*, 92, 289-300, 1993.
- 610 Estrada, M.: Primary production in the northwestern Mediterranean, *Scientia Marina*, 60, 55-64, 1996.
- 612 Fennel, K., and Boss, E.: Subsurface maxima of phytoplankton and chlorophyll: Steady-state solutions from a simple model, *Limnology and Oceanography*, 48, 1521-1534, 10.4319/lno.2003.48.4.1521, 2003.
- 614 Ferron, B., Bouruet Aubertot, P., Cuypers, Y., Schroeder, K., and Borghini, M.: How important are diapycnal mixing and geothermal heating for the deep circulation of the Western Mediterranean?, *Geophysical Research Letters*, 44, 7845-7854, 10.1002/2017gl074169, 2017.
- 616 Fisher, N. L., and Halsey, K. H.: Mechanisms that increase the growth efficiency of diatoms in low light, *Photosynthesis Research*, 129, 183-197, 10.1007/s11120-016-0282-6, 2016.
- 618 Fisher, T., Minnaard, J., and Dubinsky, Z.: Photoacclimation in the marine alga *Nannochloropsis* sp. (Eustigmatophyte): a kinetic study, *Journal of Plankton Research*, 18, 1797-1818, 10.1093/plankt/18.10.1797, 1996.
- 620 Frouin, R., Lingner, D. W., Gautier, C., Baker, K. S., and Smith, R. C.: A simple analytical formula to compute clear sky total and photosynthetically available solar irradiance at the ocean surface, *Journal of Geophysical Research: Oceans*, 94, 9731-9742, 10.1029/JC094iC07p09731, 1989.
- 622 Geider, R. J.: Light and temperature dependence of the carbon to chlorophyll a ratio in microalgae and cyanobacteria: implications for physiology and growth of phytoplankton, *New Phytologist*, 106, 1-34, 10.1111/j.1469-8137.1987.tb04788.x, 1987.
- 626 Geider, R. J.: Respiration: Taxation Without Representation?, in: *Primary Productivity and Biogeochemical Cycles in the Sea*, edited by: Falkowski, P. G., Woodhead, A. D., and Vivirito, K., Springer US, Boston, MA, 333-360, 1992.
- 628 Geider, R. J., MacIntyre, H. L., and Kana, T. M.: A dynamic model of photoadaptation in phytoplankton, *Limnology and Oceanography*, 41, 1-15, 10.4319/lno.1996.41.1.0001, 1996.
- 630 Goldman, J. C., McCarthy, J. J., and Peavey, D. G.: Growth rate influence on the chemical composition of phytoplankton in oceanic waters, *Nature*, 279, 210-215, 10.1038/279210a0, 1979.
- 632 Guieu, C., Aumont, O., Paytan, A., Bopp, L., Law, C. S., Mahowald, N., Achterberg, E. P., Marañón, E., Salihoglu, B., Crise, A., Wagener, T., Herut, B., Desboeufs, K., Kanakidou, M., Olgun, N., Peters, F., Pulido-Villena, E., Tovar-Sanchez, A., and Völker, C.: The significance of the episodic nature of atmospheric deposition to Low Nutrient Low Chlorophyll regions, *Global Biogeochemical Cycles*, 28, 1179-1198, 10.1002/2014gb004852, 2014.
- 636 Guieu, C., D'Ortenzio, F., Dulac, F., Taillandier, V., Doglioli, A., Petrenko, A., Barrillon, S., Mallet, M., Nabat, P., and Desboeufs, K.: Process studies at the air-sea interface after atmospheric deposition in the Mediterranean Sea: objectives and strategy of the PEACETIME oceanographic campaign (May–June 2017), *Biogeosciences Discuss.*, 2020, 1-65, 10.5194/bg-2020-44, 2020.
- 640 Halsey, K. H., and Jones, B. M.: Phytoplankton Strategies for Photosynthetic Energy Allocation, *Annual Review of Marine Science*, 7, 265-297, 10.1146/annurev-marine-010814-015813, 2015.
- 642 Herbrand, A., and Voituriez, B.: Hydrological structure analysis for estimating the primary production in the tropical Atlantic Ocean, *Journal of Marine Research*, 37, 87-101, 1979.
- 644 Huete-Ortega, M., Cermeño, P., Calvo-Díaz, A., and Marañón, E.: Isometric size-scaling of metabolic rate and the size abundance distribution of phytoplankton, *Proceedings of the Royal Society B: Biological Sciences*, 279, 1815-1823, [doi:10.1098/rspb.2011.2257](https://doi.org/10.1098/rspb.2011.2257), 2012.
- 646

- 648 Ignatiades, L., Gotsis-Skretas, O., Pagou, K., and Krasakopoulou, E.: Diversification of phytoplankton community structure and related parameters along a large-scale longitudinal east–west transect of the Mediterranean Sea, *Journal of Plankton Research*, 31, 411-428, 10.1093/plankt/fbn124, 2009.
- 650 Karl, D. M., Laws, E. A., Morris, P., Williams, P. J. I., and Emerson, S.: Metabolic balance of the open sea, *Nature*, 426, 32-32, 10.1038/426032a, 2003.
- 652 Kemp, A. E. S., and Villareal, T. A.: High diatom production and export in stratified waters – A potential negative feedback to global warming, *Progress in Oceanography*, 119, 4-23, <https://doi.org/10.1016/j.pocean.2013.06.004>, 2013.
- 654 Kemp, A. E. S., and Villareal, T. A.: The case of the diatoms and the muddled mandalas: Time to recognize diatom adaptations to stratified waters, *Progress in Oceanography*, 167, 138-149, <https://doi.org/10.1016/j.pocean.2018.08.002>, 2018.
- 656
- Kirchman, D. L.: Calculating microbial growth rates from data on production and standing stocks, *Marine Ecology Progress Series*, 233, 303-306, 2002.
- 668
- Kremer, C. T., Thomas, M. K., and Litchman, E.: Temperature- and size-scaling of phytoplankton population growth rates: Reconciling the Eppley curve and the metabolic theory of ecology, *Limnology and Oceanography*, 62, 1658-1670, 10.1002/lno.10523, 2017.
- 660
- Lande, R., and Wood, A. M.: Suspension times of particles in the upper ocean, *Deep Sea Research Part A. Oceanographic Research Papers*, 34, 61-72, [https://doi.org/10.1016/0198-0149\(87\)90122-1](https://doi.org/10.1016/0198-0149(87)90122-1), 1987.
- 662
- Landry, M. R., Brown, S. L., Rii, Y. M., Selph, K. E., Bidigare, R. R., Yang, E. J., and Simmons, M. P.: Depth-stratified phytoplankton dynamics in Cyclone Opal, a subtropical mesoscale eddy, *Deep Sea Research Part II: Topical Studies in Oceanography*, 55, 1348-1359, <https://doi.org/10.1016/j.dsr2.2008.02.001>, 2008.
- 664
- Landry, M. R., Ohman, M. D., Goericke, R., Stukel, M. R., and Tsyrklevich, K.: Lagrangian studies of phytoplankton growth and grazing relationships in a coastal upwelling ecosystem off Southern California, *Progress in Oceanography*, 83, 208-216, <https://doi.org/10.1016/j.pocean.2009.07.026>, 2009.
- 666
- Larsen, A., Castberg, T., Sandaa, R. A., Brussaard, C. P. D., Egge, J., Heldal, M., Paulino, A., Thyrrhaug, R., Hannen, E. J. v., and Bratbak, G.: Population dynamics and diversity of phytoplankton, bacteria and viruses in a seawater enclosure, *Marine Ecology Progress Series*, 221, 47-57, 2001.
- 670
- 672
- Lavigne, H., D'Ortenzio, F., Ribera D'Alcalà, M., Claustre, H., Sauzède, R., and Gacic, M.: On the vertical distribution of the chlorophyll *a* concentration in the Mediterranean Sea: a basin-scale and seasonal approach, *Biogeosciences*, 12, 5021-5039, 10.5194/bg-12-5021-2015, 2015.
- 674
- 676
- 678
- Lemée, R., Rochelle-Newall, E., Wambeke, F. V., Pizay, M. D., Rinaldi, P., and Gattuso, J. P.: Seasonal variation of bacterial production, respiration and growth efficiency in the open NW Mediterranean Sea, *Aquatic Microbial Ecology*, 29, 227-237, 2002.
- Letelier, R. M., Karl, D. M., Abbott, M. R., and Bidigare, R. R.: Light driven seasonal patterns of chlorophyll and nitrate in the lower euphotic zone of the North Pacific Subtropical Gyre, *Limnology and Oceanography*, 49, 508-519, 10.4319/lo.2004.49.2.0508, 2004.
- 680
- 682
- López-Sandoval, D. C., Fernández, A., and Marañón, E.: Dissolved and particulate primary production along a longitudinal gradient in the Mediterranean Sea, *Biogeosciences*, 8, 815-825, 10.5194/bg-8-815-2011, 2011.
- 684
- 686
- MacIntyre, H. L., Kana, T. M., Anning, T., and Geider, R. J.: Photoacclimation of photosynthesis irradiance response curves and photosynthetic pigments in microalgae and cyanobacteria, *Journal of Phycology*, 38, 17-38, 10.1046/j.1529-8817.2002.00094.x, 2002.
- Magazzù, G., and Decembrini, F.: Primary production, biomass and abundance of phototrophic picoplankton in the Mediterranean Sea: a review, *Aquatic Microbial Ecology*, 09, 97-104, 1995.
- 688
- Marañón, E., Holligan, P. M., Varela, M., Mouriño, B., and Bale, A. J.: Basin-scale variability of phytoplankton biomass, production and growth in the Atlantic Ocean, *Deep Sea Research Part I: Oceanographic Research Papers*, 47, 825-857, [https://doi.org/10.1016/S0967-0637\(99\)00087-4](https://doi.org/10.1016/S0967-0637(99)00087-4), 2000.
- 690

- 692 Marañón, E., Cermeño, P., Fernández, E., Rodríguez, J., and Zabala, L.: Significance and mechanisms of photosynthetic
694 production of dissolved organic carbon in a coastal eutrophic ecosystem, *Limnology and Oceanography*, 49, 1652-1666,
10.4319/lo.2004.49.5.1652, 2004.
- Marañón, E.: Phytoplankton growth rates in the Atlantic subtropical gyres, *Limnology and Oceanography*, 50, 299-310,
696 10.4319/lo.2005.50.1.0299, 2005.
- Marañón, E., Fernández, A., Mouriño-Carballido, B., Martínez-García, S., Teira, E., Cermeño, P., Chouciño, P., Huete-
698 Ortega, M., Fernández, E., Calvo-Díaz, A., Morán, X. A. G., Bode, A., Moreno-Ostos, E., Varela, M. M., Patey, M. D.,
and Achterberg, E. P.: Degree of oligotrophy controls the response of microbial plankton to Saharan dust, *Limnology
700 and Oceanography*, 55, 2339-2352, 10.4319/lo.2010.55.6.2339, 2010.
- Marañón, E., Cermeño, P., López-Sandoval, D. C., Rodríguez-Ramos, T., Sobrino, C., Huete-Ortega, M., Blanco, J. M.,
702 and Rodríguez, J.: Unimodal size scaling of phytoplankton growth and the size dependence of nutrient uptake and use,
Ecology Letters, 16, 371-379, 10.1111/ele.12052, 2013.
- Marañón, E., Cermeño, P., Huete-Ortega, M., López-Sandoval, D. C., Mouriño-Carballido, B., and Rodríguez-Ramos,
704 T.: Resource Supply Overrides Temperature as a Controlling Factor of Marine Phytoplankton Growth, *PLOS ONE*, 9,
706 e99312, 10.1371/journal.pone.0099312, 2014.
- Marañón, E.: Cell Size as a Key Determinant of Phytoplankton Metabolism and Community Structure, *Annual Review
708 of Marine Science*, 7, 241-264, 10.1146/annurev-marine-010814-015955, 2015.
- Marañón, E., Lorenzo, M. P., Cermeño, P., and Mouriño-Carballido, B.: Nutrient limitation suppresses the temperature
710 dependence of phytoplankton metabolic rates, *The ISME Journal*, 12, 1836-1845, 10.1038/s41396-018-0105-1, 2018.
- Marie, D., Simon, N., Guillou, L., Partensky, F., and Vaulot, D.: Flow Cytometry Analysis of Marine Picoplankton, in:
712 *In Living Color: Protocols in Flow Cytometry and Cell Sorting*, edited by: Diamond, R. A., and Demaggio, S., Springer
Berlin Heidelberg, Berlin, Heidelberg, 421-454, 2000.
- Martínez-Vicente, V., Dall'Olmo, G., Tarran, G., Boss, E., and Sathyendranath, S.: Optical backscattering is correlated
714 with phytoplankton carbon across the Atlantic Ocean, *Geophysical Research Letters*, 40, 1154-1158, 10.1002/grl.50252,
716 2013.
- Marty, J.-C., and Chiavérini, J.: Seasonal and interannual variations in phytoplankton production at DYFAMED time-
718 series station, northwestern Mediterranean Sea, *Deep Sea Research Part II: Topical Studies in Oceanography*, 49, 2017-
2030, [https://doi.org/10.1016/S0967-0645\(02\)00025-5](https://doi.org/10.1016/S0967-0645(02)00025-5), 2002.
- Marty, J.-C., Chiavérini, J., Pizay, M.-D., and Avril, B.: Seasonal and interannual dynamics of nutrients and
720 phytoplankton pigments in the western Mediterranean Sea at the DYFAMED time-series station (1991–1999), *Deep
722 Sea Research Part II: Topical Studies in Oceanography*, 49, 1965-1985, [https://doi.org/10.1016/S0967-0645\(02\)00022-
X](https://doi.org/10.1016/S0967-0645(02)00022-X), 2002.
- Mena, C., Reglero, P., Hidalgo, M., Sintés, E., Santiago, R., Martín, M., Moyà, G., and Balbín, R.: Phytoplankton
724 Community Structure Is Driven by Stratification in the Oligotrophic Mediterranean Sea, *Frontiers in Microbiology*, 10,
726 10.3389/fmicb.2019.01698, 2019.
- Mignot, A., Claustre, H., Uitz, J., Poteau, A., D'Ortenzio, F., and Xing, X.: Understanding the seasonal dynamics of
728 phytoplankton biomass and the deep chlorophyll maximum in oligotrophic environments: A Bio-Argo float
investigation, *Global Biogeochemical Cycles*, 28, 856-876, 10.1002/2013gb004781, 2014.
- Mills, M. M., Ridame, C., Davey, M., La Roche, J., and Geider, R. J.: Iron and phosphorus co-limit nitrogen fixation in
730 the eastern tropical North Atlantic, *Nature*, 429, 292-294, 10.1038/nature02550, 2004.
- Moberg, E. A., and Sosik, H. M.: Distance maps to estimate cell volume from two-dimensional plankton images,
732 *Limnology and Oceanography: Methods*, 10, 278-288, 10.4319/lom.2012.10.278, 2012.
- Mobley, C. D., and Boss, E. S.: Improved irradiances for use in ocean heating, primary production, and photo-oxidation
734 calculations, *Appl. Opt.*, 51, 6549-6560, 10.1364/AO.51.006549, 2012.
- Moore, C. M., Mills, M. M., Arrigo, K. R., Berman-Frank, I., Bopp, L., Boyd, P. W., Galbraith, E. D., Geider, R. J.,
736 Guieu, C., Jaccard, S. L., Jickells, T. D., La Roche, J., Lenton, T. M., Mahowald, N. M., Marañón, E., Marinov, I.,

- 738 Moore, J. K., Nakatsuka, T., Oschlies, A., Saito, M. A., Thingstad, T. F., Tsuda, A., and Ulloa, O.: Processes and patterns of oceanic nutrient limitation, *Nature Geoscience*, 6, 701-710, 10.1038/ngeo1765, 2013.
- 740 Morán, X. A. G., Estrada, M., Gasol, J. M., and Pedrós-Alió, C.: Dissolved Primary Production and the Strength of Phytoplankton– Bacterioplankton Coupling in Contrasting Marine Regions, *Microbial Ecology*, 44, 217-223, 10.1007/s00248-002-1026-z, 2002.
- 742
- Morán, X. A. G., and Alonso-Sáez, L.: Independence of bacteria on phytoplankton? Insufficient support for Fouilland & Mostajir's (2010) suggested new concept, *FEMS Microbiology Ecology*, 78, 203-205, 10.1111/j.1574-6941.2011.01167.x, 2011.
- 744
- Morel, A., and Berthon, J.-F.: Surface pigments, algal biomass profiles, and potential production of the euphotic layer: Relationships reinvestigated in view of remote-sensing applications, *Limnology and Oceanography*, 34, 1545-1562, 10.4319/lo.1989.34.8.1545, 1989.
- 746
- 748
- Moutin, T., and Raimbault, P.: Primary production, carbon export and nutrients availability in western and eastern Mediterranean Sea in early summer 1996 (MINOS cruise), *Journal of Marine Systems*, 33-34, 273-288, [https://doi.org/10.1016/S0924-7963\(02\)00062-3](https://doi.org/10.1016/S0924-7963(02)00062-3), 2002.
- 750
- O'Connor, M. I., Piehler, M. F., Leech, D. M., Anton, A., and Bruno, J. F.: Warming and Resource Availability Shift Food Web Structure and Metabolism, *PLOS Biology*, 7, e1000178, 10.1371/journal.pbio.1000178, 2009.
- 752
- Olofsson, M., Robertson, E. K., Edler, L., Arneborg, L., Whitehouse, M. J., and Ploug, H.: Nitrate and ammonium fluxes to diatoms and dinoflagellates at a single cell level in mixed field communities in the sea, *Scientific Reports*, 9, 1424, 10.1038/s41598-018-38059-4, 2019.
- 754
- 756
- Olson, R. J., and Sosik, H. M.: A submersible imaging-in-flow instrument to analyze nano-and microplankton: Imaging FlowCytobot, *Limnology and Oceanography: Methods*, 5, 195-203, 10.4319/lom.2007.5.195, 2007.
- 758
- Pan, Y., Rao, D. V. S., and Mann, K. H.: Acclimation to low light intensity in photosynthesis and growth of *Pseudonitzschia multiseris* Hasle, a neurotoxic diatom, *Journal of Plankton Research*, 18, 1427-1438, 10.1093/plankt/18.8.1427, 1996.
- 760
- 762
- 764
- Pedrós-Alió, C., Calderón-Paz, J.-I., Guixa-Boixereu, N., Estrada, M., and Gasol, J. M.: Bacterioplankton and phytoplankton biomass and production during summer stratification in the northwestern Mediterranean Sea, *Deep Sea Research Part I: Oceanographic Research Papers*, 46, 985-1019, [https://doi.org/10.1016/S0967-0637\(98\)00106-X](https://doi.org/10.1016/S0967-0637(98)00106-X), 1999.
- Pérez, V., Fernández, E., Marañón, E., Morán, X. A. G., and Zubkov, M. V.: Vertical distribution of phytoplankton biomass, production and growth in the Atlantic subtropical gyres, *Deep Sea Research Part I: Oceanographic Research Papers*, 53, 1616-1634, <https://doi.org/10.1016/j.dsr.2006.07.008>, 2006.
- 766
- 768
- 770
- Pulido-Villena, E., Ghiglione, J. F., Ortega-Retuerta, E., Van Wambeke, F., and Zohary, T.: Heterotrophic bacteria in the pelagic realm of the Mediterranean Sea, in: *Life in the Mediterranean Sea: A Look at Habitat Changes*, edited by: Stambler, N., Nova Science Publishers, Inc., 2012.
- Ras, J., Claustre, H., and Uitz, J.: Spatial variability of phytoplankton pigment distributions in the Subtropical South Pacific Ocean: comparison between in situ and predicted data, *Biogeosciences*, 5, 353-369, 10.5194/bg-5-353-2008, 2008.
- 772
- 774
- 776
- Robinson, A., Bouman, H. A., Tilstone, G. H., and Sathyendranath, S.: Size Class Dependent Relationships between Temperature and Phytoplankton Photosynthesis-Irradiance Parameters in the Atlantic Ocean, *Frontiers in Marine Science*, 4, 10.3389/fmars.2017.00435, 2018.
- Siokou-Frangou, I., Christaki, U., Mazzocchi, M. G., Montresor, M., Ribera d'Alcalá, M., Vaqué, D., and Zingone, A.: Plankton in the open Mediterranean Sea: a review, *Biogeosciences*, 7, 1543-1586, 10.5194/bg-7-1543-2010, 2010.
- Smith, D. C., and Azam, F.: A simple, economical method for measuring bacterial protein synthesis rates in seawater using 3H-leucine, *Marine Microbial Food Webs*, 6, 107-114, 1992.
- 780
- Steele, J.: A study of production in the Gulf of Mexico, *Journal of Marine Research*, 3, 211-222, 1964.

782 Steinberg, D. K., Carlson, C. A., Bates, N. R., Johnson, R. J., Michaels, A. F., and Knap, A. H.: Overview of the US
784 JGOFS Bermuda Atlantic Time-series Study (BATS): a decade-scale look at ocean biology and biogeochemistry, *Deep
Sea Research Part II: Topical Studies in Oceanography*, 48, 1405-1447, [https://doi.org/10.1016/S0967-0645\(00\)00148-
X](https://doi.org/10.1016/S0967-0645(00)00148-X), 2001.

786 Taillandier, V., Prieur, L., D'Ortenzio, F., Ribera d'Alcalà, M., and Pulido-Villena, E.: Profiling float observation of
788 thermohaline staircases in the western Mediterranean Sea and impact on nutrient fluxes, *Biogeosciences Discuss.*, 2020,
1-43, 10.5194/bg-2019-504, 2020.

790 Tanaka, T., Thingstad, T. F., Christaki, U., Colombet, J., Cornet-Barthaux, V., Courties, C., Grattepanche, J. D.,
792 Lagaria, A., Nedoma, J., Oriol, L., Psarra, S., Pujo-Pay, M., and Van Wambeke, F.: Lack of P-limitation of
phytoplankton and heterotrophic prokaryotes in surface waters of three anticyclonic eddies in the stratified
Mediterranean Sea, *Biogeosciences*, 8, 525-538, 10.5194/bg-8-525-2011, 2011.

794 Tsiola, A., Pitta, P., Fodelianakis, S., Pete, R., Magiopoulos, I., Mara, P., Psarra, S., Tanaka, T., and Mostajir, B.:
Nutrient Limitation in Surface Waters of the Oligotrophic Eastern Mediterranean Sea: an Enrichment Microcosm
Experiment, *Microbial Ecology*, 71, 575-588, 10.1007/s00248-015-0713-5, 2016.

796 Turley, C. M., Bianchi, M., Christaki, U., Conan, P., Harris, J. R. W., Psarra, S., Ruddy, G., Stutt, E. D., Tselepidis, A.,
798 and Wambeke, F. V.: Relationship between primary producers and bacteria in an oligotrophic sea--the Mediterranean
and biogeochemical implications, *Marine Ecology Progress Series*, 193, 11-18, 2000.

800 Uitz, J., Claustre, H., Morel, A., and Hooker, S. B.: Vertical distribution of phytoplankton communities in open ocean:
An assessment based on surface chlorophyll, *Journal of Geophysical Research: Oceans*, 111, 10.1029/2005jc003207,
2006.

802 Uitz, J., Huot, Y., Bruyant, F., Babin, M., and Claustre, H.: Relating phytoplankton photophysiological properties to
community structure on large scales, *Limnology and Oceanography*, 53, 614-630, 10.4319/lo.2008.53.2.0614, 2008.

804 Uitz, J., Claustre, H., Gentili, B., and Stramski, D.: Phytoplankton class-specific primary production in the world's
oceans: Seasonal and interannual variability from satellite observations, *Global Biogeochemical Cycles*, 24,
806 10.1029/2009gb003680, 2010.

808 Uitz, J., Stramski, D., Gentili, B., D'Ortenzio, F., and Claustre, H.: Estimates of phytoplankton class-specific and total
primary production in the Mediterranean Sea from satellite ocean color observations, *Global Biogeochemical Cycles*,
26, 10.1029/2011gb004055, 2012.

810 Van Wambeke, F., Heussner, S., Diaz, F., Raimbault, P., and Conan, P.: Small-scale variability in the
812 coupling/uncoupling of bacteria, phytoplankton and organic carbon fluxes along the continental margin of the Gulf of
Lions, Northwestern Mediterranean Sea, *Journal of Marine Systems*, 33-34, 411-429, [https://doi.org/10.1016/S0924-
7963\(02\)00069-6](https://doi.org/10.1016/S0924-7963(02)00069-6), 2002.

814 Van Wambeke, F., Pulido, E., Dinasquet, J., Djaoudi, K., Engel, A., Garel, M., Guasco, S., Nunige, S., Taillandier, V.,
816 Zäncker, B., and Tamburini, C.: Spatial patterns of biphasic ectoenzymatic kinetics related to biogeochemical properties
in the Mediterranean Sea, *Biogeosciences Discuss.*, 2020, 1-38, 10.5194/bg-2020-253, 2020a.

818 Van Wambeke, F., Taillandier, V., Deboeufs, K., Pulido-Villena, E., Dinasquet, J., Engel, A., Marañón, E., Ridame, C.,
and Guieu, C.: Influence of atmospheric deposition on biogeochemical cycles in an oligotrophic ocean system,
Biogeosciences Discuss., 2020, 1-51, 10.5194/bg-2020-411, 2020b.

820 Veldhuis, M. J. W., and Kraay, G. W.: Phytoplankton in the subtropical Atlantic Ocean: towards a better assessment of
822 biomass and composition, *Deep Sea Research Part I: Oceanographic Research Papers*, 51, 507-530,
<https://doi.org/10.1016/j.dsr.2003.12.002>, 2004.

824 Villareal, T. A., Woods, S., Moore, J. K., and CulverRymysza, K.: Vertical migration of *Rhizosolenia* mats and their
significance to NO₃⁻ fluxes in the central North Pacific gyre, *Journal of Plankton Research*, 18, 1103-1121,
10.1093/plankt/18.7.1103, 1996.

826 Wang, Q., Lyu, Z., Omar, S., Cornell, S., Yang, Z., and Montagnes, D. J. S.: Predicting temperature impacts on aquatic
828 productivity: Questioning the metabolic theory of ecology's "canonical" activation energies, *Limnology and
Oceanography*, 64, 1172-1185, 10.1002/lno.11105, 2019.

830 Yoon, J. E., Yoo, K. C., Macdonald, A. M., Yoon, H. I., Park, K. T., Yang, E. J., Kim, H. C., Lee, J. I., Lee, M. K.,
Jung, J., Park, J., Lee, J., Kim, S., Kim, S. S., Kim, K., and Kim, I. N.: Reviews and syntheses: Ocean iron fertilization
832 experiments – past, present, and future looking to a future Korean Iron Fertilization Experiment in the Southern Ocean
(KIFES) project, *Biogeosciences*, 15, 5847-5889, 10.5194/bg-15-5847-2018, 2018.

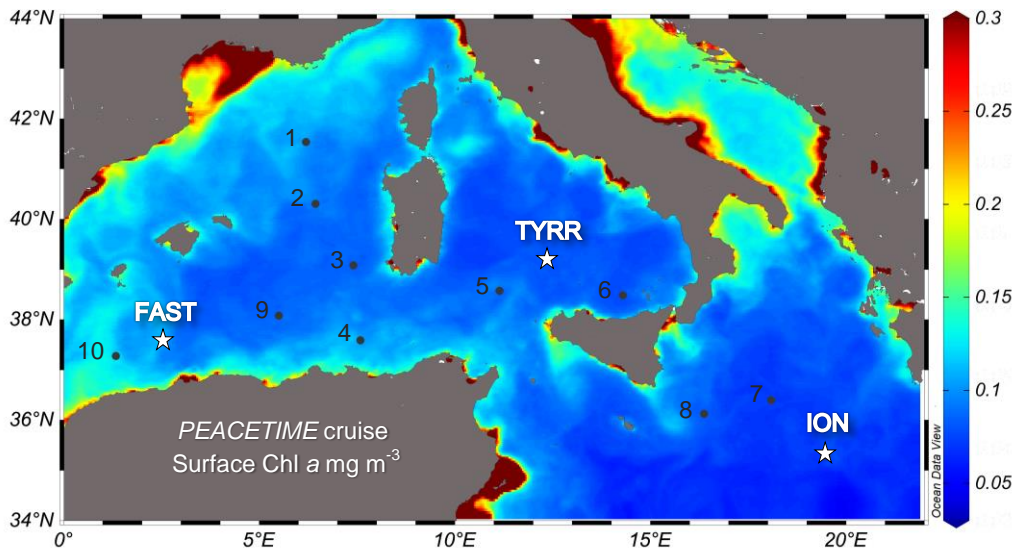
834 Zäncker, B., Cunliffe, M., and Engel, A.: Eukaryotic community composition in the sea surface microlayer across an
east-west transect in the Mediterranean Sea, *Biogeosciences Discuss.*, 2020, 1-20, 10.5194/bg-2020-249, 2020.

836 **Table 1.** Mean and standard deviation (in brackets) for different physical, chemical and biological variables at the three
838 long stations. N is the Brunt-Väisälä frequency. Nitracline depth is the first depth at which nitrate concentration reached
840 $0.5 \mu\text{mol L}^{-1}$ while phosphacline depth corresponds to the first depth at which phosphate concentration reached $0.03 \mu\text{mol L}^{-1}$. Chlorophyll *a* concentration and particulate primary production (PP) were integrated from the surface to the
842 1% PAR depth. Heterotrophic prokaryotic production (BP) was integrated from the surface to 200 m. IFCB is Imaging
Flow CytoBot and ESD is Equivalent Spherical Diameter. See Methods for details.

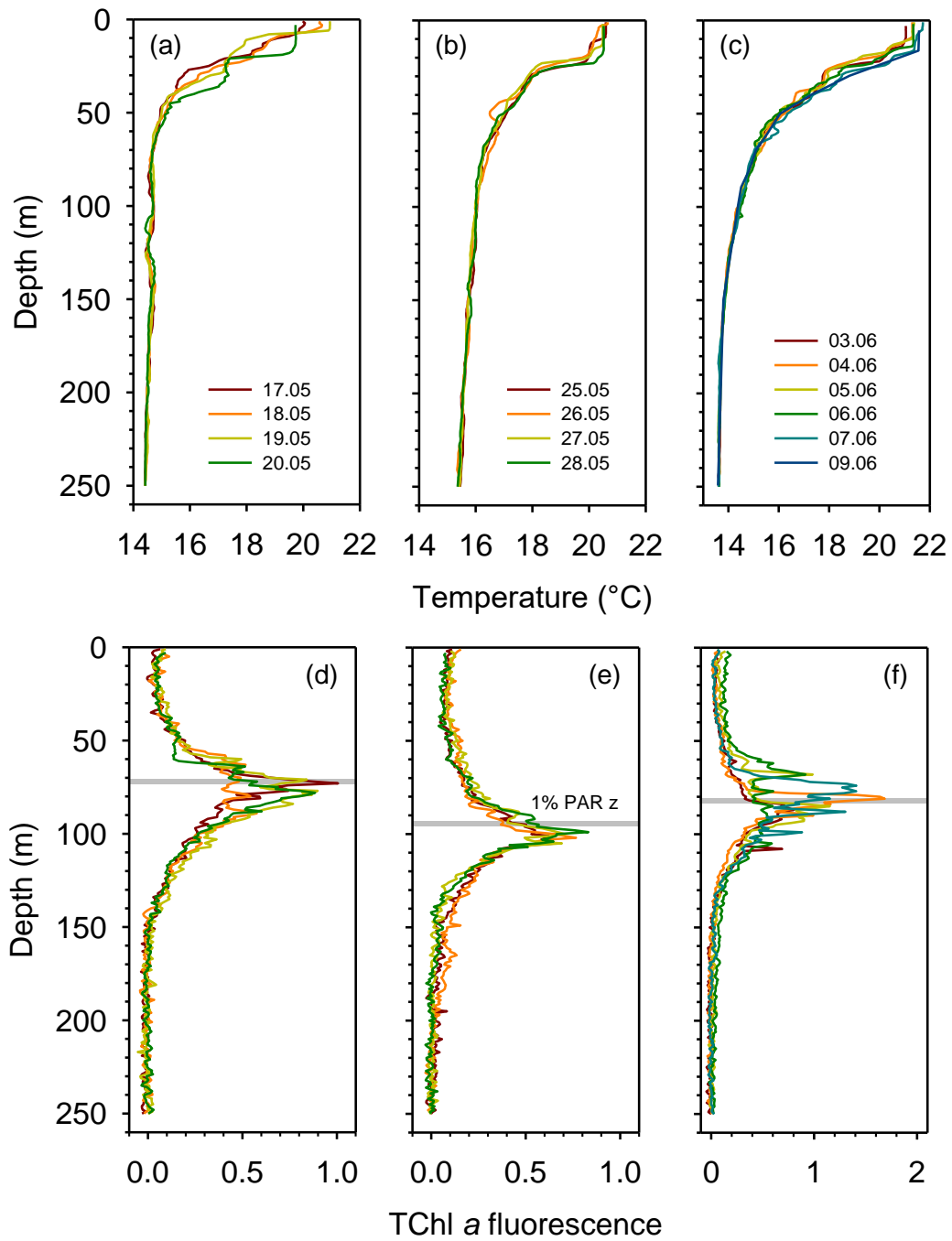
Variable	TYRR	ION	FAST
Surface temperature (°C)	20.1 (0.6)	20.4 (0.1)	21.4 (0.2)
<u>Depth of maximum N (m)</u>	<u>14 (8)</u>	<u>23 (2)</u>	<u>22 (3)</u>
Surface TChl <i>a</i> (mg m ⁻³)	0.07 (0.01)	0.07 (0.01)	0.08 (0.01)
Nitracline depth (m)	71 (3)	105 (2)	78 (8)
Phosphacline depth (m)	86 (3)	181 (7)	90 (5)
DCM depth (m)	74 (4)	96 (4)	85 (6)
1% PAR depth (m)	71 (8)	94 (6)	81 (5)
0.3 mol m ⁻² d ⁻¹ isolume depth (m)	80 (7)	104 (5)	91 (6)
PAR at DCM (mol m ⁻² d ⁻¹)	0.47 (0.26)	0.45 (0.06)	0.44 (0.19)
DCM TChl <i>a</i> concentration (mg m ⁻³)	0.57 (0.11)	0.57 (0.07)	0.62 (0.29)
Surface phytoplankton biomass (mgC m ⁻³)	6 (1)	6 (1)	5 (2)
DCM phytoplankton biomass (mgC m ⁻³)	13 5 (8)	14 1 (1)	16 (10)
Surface C:Chl <i>a</i> ratio (g:g)	97 83 (87)	91 84 (57)	89 67 (230)
DCM C:Chl <i>a</i> ratio (g:g)	27 5 (408)	24 3 (42)	34 28 (81)
Surface Fucoxanthin:TChl <i>a</i> ratio	0.036 (0.001)	0.040 (0.004)	0.051 (0.005)
DCM Fucoxanthin:TChl <i>a</i> ratio	0.21 (0.04)	0.29 (0.03)	0.24 (0.10)
<u>DCM cell biovolume from IFCB ($\mu\text{m}^3 \text{cell}^{-1}$)</u>	<u>78 (37)</u>	<u>72 (35)</u>	<u>73 (12)</u>
<u>DCM % Phytoplankton C > 5 μm in ESD</u>	<u>59 (16)</u>	<u>73 (2)</u>	<u>66 (11)</u>
<u>DCM % PP > 2 μm in ESD</u>	<u>74 (6)</u>	<u>81 (6)</u>	<u>73 (9)</u>
Integrated TChl <i>a</i> (mg m ⁻²) (0 - 1% PAR z)	16 (2)	18 (2)	21 (9)
Integrated PP (mgC m ⁻² d ⁻¹) (0 - 1% PAR z)	170 (36)	186 (56)	209 (67)
% integrated PP > 2 μm (0 - 1% PAR z)	72 (4)	75 (6)	73 (3)
Integrated BP (mgC m ⁻² d ⁻¹) (0 - 200 m)	57 (3)	51 (9)	89 (10)

Table 2. Estimation of the contribution of nutrient diffusive fluxes to sustain the requirements of the deep phytoplankton biomass maximum (DPBM) in stations TYRR and FAST. The DPBM layer considered has a thickness of 30 m and the nutrient requirements of primary production are assumed to follow Redfield C:N:P proportions. The magnitude of nitrate and phosphate diffusive fluxes at the base of the DBM is taken from Taillandier et al. (2020).

	TYRR	FAST
Mean phytoplankton concentration (mgC m ⁻³)	15	10
Biomass turnover rate (d ⁻¹)	0.3	0.3
C:N molar ratio of phytoplankton biomass	6.6	6.6
C:P molar ratio of phytoplankton biomass	106	106
Vertical extent of DPBM layer (m)	30	30
Lower limit of deep biomass layer (m)	60	80
N requirement of DPBM (μmol N m ⁻² d ⁻¹)	1705	1136
P requirement of DPBM (μmol P m ⁻² d ⁻¹)	107	71
Diffusive N flux (Taillandier et al. 2020) (μmol N m ⁻² d ⁻¹)	560	101
Diffusive P flux (Taillandier et al. 2020) (μmol P m ⁻² d ⁻¹)	12.8	2.3
% of N requirement met by diffusive flux	33	9
% of P requirement met by diffusive flux	12	3

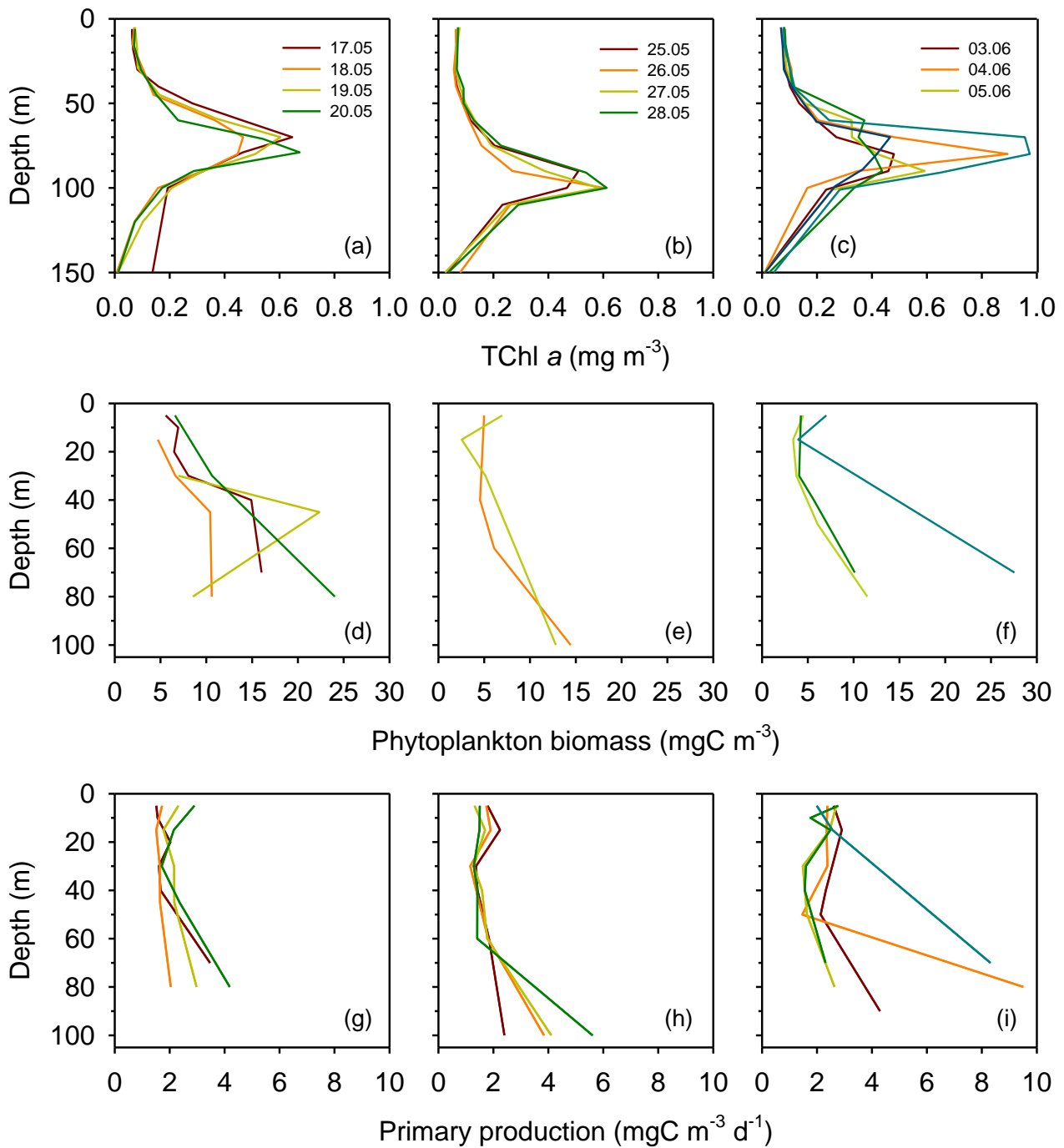


852 **Figure 1.** Location of the sampled stations superimposed on a map of ocean colour-based surface chlorophyll *a*
 854 concentration (mg m^{-3}) averaged over the period of the PEACETIME cruise (12 May – 8 June 2017). Dots and stars
 indicate the location of short and long stations, respectively. Ocean colour data from MODIS/Aqua, NASA Goddard
 Space Flight Center.



856

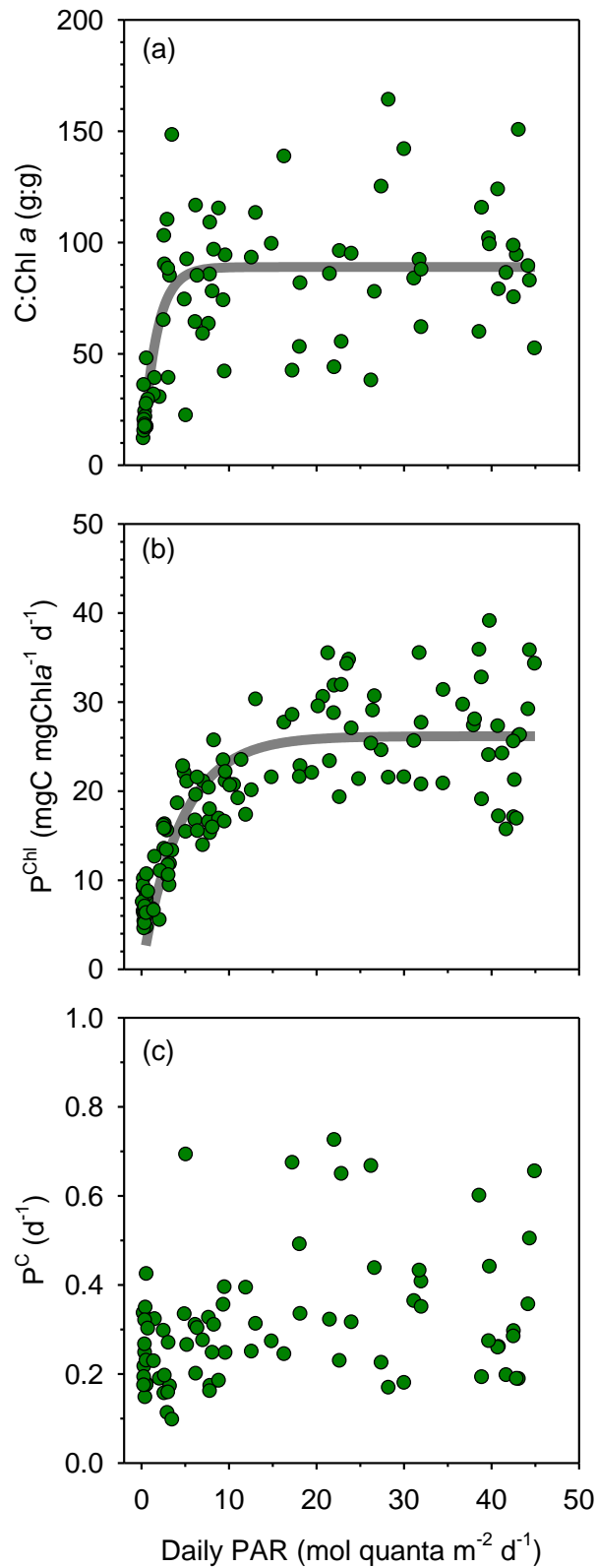
858 **Figure 2.** Vertical profiles of temperature and fluorescence (0-250 m) during each sampling day at the long stations
 860 TYRR (a, c), ION (b, e) and FAST (c, f). The colour code denotes the sampling date in dd.mm format, and the grey bars
 indicate the mean value of the 1% PAR depth at each station. The fluorescence signal was calibrated against HPLC-
 determined total chlorophyll *a* concentration.



862

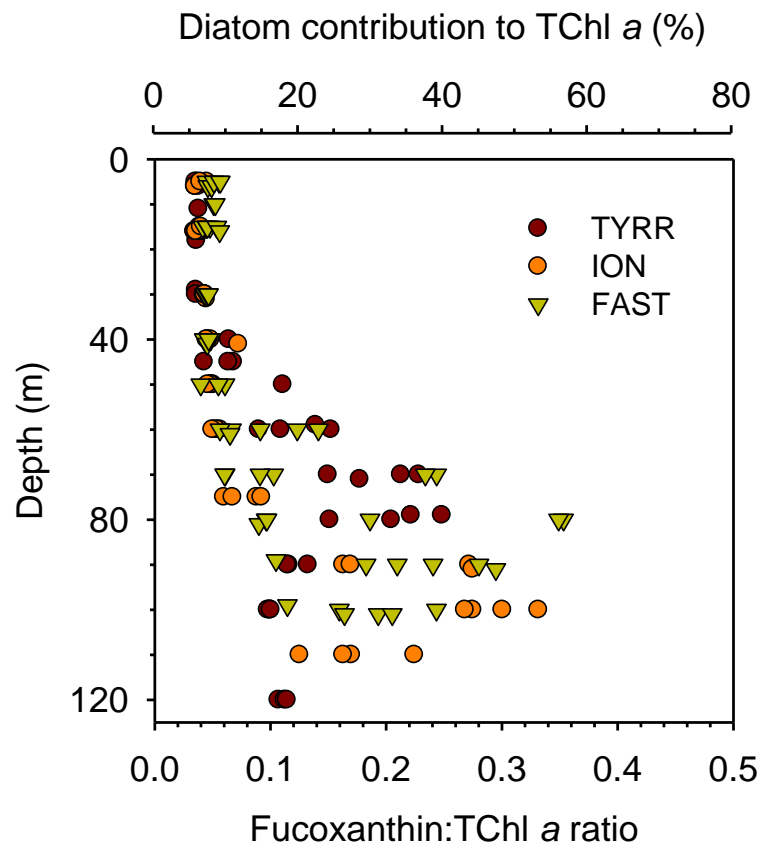
864

Figure 3. Vertical profiles of total chlorophyll *a* concentration (a,b,c), phytoplankton biomass concentration (d,e,f) and primary production (g,h,i) during each sampling day at the long stations TYRR (a,d,g), ION (b,e,h) and FAST (c,f,i).

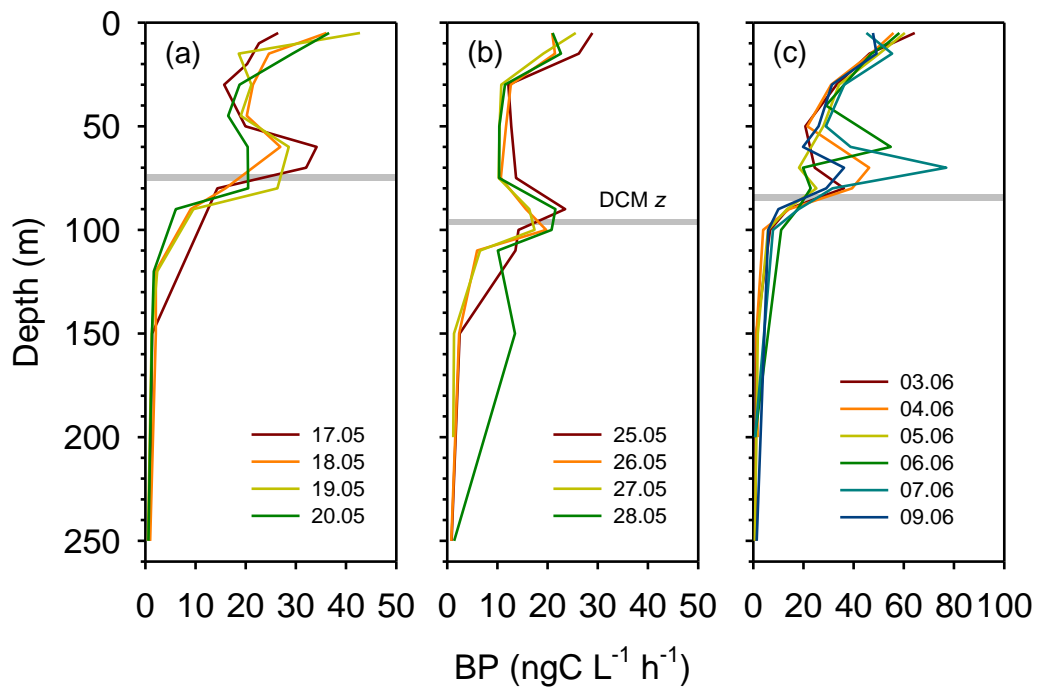


866

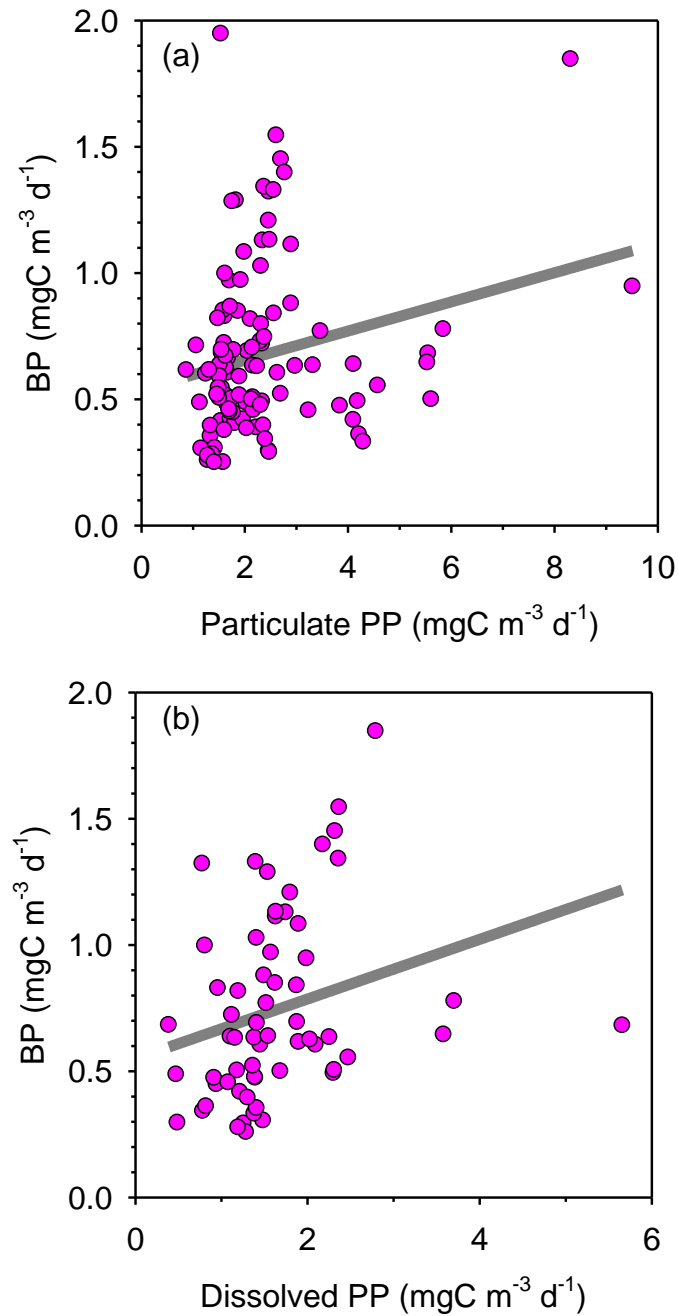
868 **Figure 4.** Relationship between PAR and a) phytoplankton carbon to chlorophyll *a* ratio, b) chlorophyll *a*-specific
 870 particulate primary production and c) phytoplankton biomass turnover rate with data from all stations pooled together.
 The non linear fits are (a) $y = 92.789.0 (1 - \exp(-0.624 x))$, $r^2 = 0.4853$, $p < 0.001$, $n = 6976$ and (b) $y = 26.2 (1 - \exp(-0.22 x))$, $r^2 = 0.68$, $p < 0.001$, $n = 119$.



876 **Figure 5.** Vertical variability of the fucoxanthin to total chlorophyll *a* concentration ratio in the three long stations. The
 878 upper *x*-axis is included as a reference and shows the estimated diatom contribution to TChl *a* computed with the mean
 value of three different conversion factors. See Methods for details.



880 **Figure 6.** Vertical profiles of heterotrophic prokaryotic production (BP, dawn casts only) during each sampling day at the long-term stations a) TYRR, b) ION and c) and FAST. The grey line indicates depth of the DCM at each station.



882

884

Figure 7. Bacterial production as a function of a) particulate and b) dissolved primary production with data from all stations pooled together. The linear regression models are (a) $y = 0.058x + 0.54$ ($r^2 = 0.05$, $n = 110$, $p = 0.016$) and (b) $y = 0.12x + 0.55$ ($r^2 = 0.07$, $n = 62$, $p = 0.034$).